AUSTRALIAN NUCLEAR SCIENCE AND TECHNOLOGY ORGANISATION

LUCAS HEIGHTS RESEARCH LABORATORIES

FINAL REPORT FOR AWRAC PROJECT 85/05

ON

IRON AND MANGANESE REMOVAL FROM WATER SUPPLIES

by

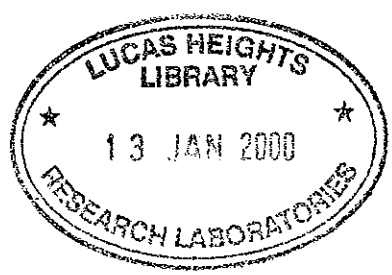

T.D. WAITE

Environmental Science Program

December 1990

ISBN 0 642-59910-6

ISSN 1030-7745

The following descriptors have been assigned from the INIS Thesaurus to describe the subject content of this report for information retrieval purposes. For further details please refer to IAEA-INIA 12 (INIS: Manual for Indexing) and IAEA-INIS-13 (INIS: Thesaurus published in Vienna by the International Atomic Energy Agency.

ANSTO; AUSTRALIA; CONTAMINATION; ENVIRONMENT; FRESHWATER; POTABLE WATER; WATER SUPPLY; WATER TREATMENT; IRON; MANGANESE; OXIDATION; AGGREGATION; FLOCCULATION; FILTRATION; OPTIMISATION; DRINKING WATER.

EDITORIAL NOTE

The Australian Nuclear Science and Technology Organisation (ANSTO) replaced the Australian Nuclear Energy Commission (AAEC) on 27 April 1987. Reports issued after April 1987 have the prefix ANSTO with no change of the symbol (E,M, S or C) or numbering sequence.

Table of Contents

ACKNOWLEDGEMENTS

This report represents the contribution of a number of research personnel. Ms Janice A. Stubbings provided essential conceptual and experimental input throughout the project and contributed particularly in initial interaction with the Wyong Shire Council and in developing our expertise in application of photon correlation spectrometry (PCS) to particle sizing. Ms Rose Amal and Ms Michelle Markham, vacation employees at ANSTO and supported by AWRAC, extended the application of PCS to investigation of aggregation of colloidal iron and manganese oxides. Ms Robyn Walton, also an AWRAC sponsored vacation employee, contributed to our understanding of the kinetics of oxidation of manganese (II) by chlorine and potassium permanganate.

Wyong Shire Council personnel provided invaluable support throughout the project. The contribution and encouragement of Mr Michael Boake, Project Engineer at Wyong, is particularly acknowledged.

The friendship and advice of Drs Barry Chiswell, David Dixon and Lindsay Sly - coparticipants on a National Advisory Committee on Iron and Manganese established through the course of this project - is gratefully acknowledged.

1 INTRODUCTION

1.1 Project Overview and Report Synopsis

The objective of this research project is the examination of the major factors governing the efficiency of removal of iron and manganese from water supplies. This objective has been met through a multi-faceted study involving the following major components:

- review of problems created by iron and manganese in Australian water supplies with particular reference to selected water sources;
- review of methods used for removal of iron and manganese from water supplies;
- detailed laboratory studies of the critical processes of Fe(II) and Mn(II) oxidation, iron and manganese oxide aggregation (coagulation/flocculation) and particle removal by filtration.

The process studies indicated above have been undertaken under both simple, idealised conditions (i.e. using well characterised particulate oxides and relatively simple solution conditions) and under conditions more typical of a water treatment plant. The latter studies have been undertaken for the most part using the waters of Mardi Dam in the New South Wales shire of Wyong.

In this report, the reviews of problems caused by iron and manganese and the methods available for the removal of these elements from water supplies are documented in the main body of the report. Particularly extensive studies have been undertaken of the aggregation of colloidal oxides and methods used and results of studies undertaken under relatively simple, well defined conditions are given in Appendix 1.

1.2 Iron and Manganese in Australian Water Supplies

Both manganese (Mn) and iron (Fe) cause serious problems in potable and industrial water systems when present in excessive concentrations. While there is no evidence that the presence of manganese and iron in drinking waters is detrimental to human health, these substances generate extensive "dirty water" problems on oxidation from the soluble reduced forms to the particulate oxidized states. Manganese is often particularly troublesome due to the slow rate of oxygen or chlorine induced oxidation and the necessity for use of more powerful oxidants within the treatment plant. On entering the distribution system, manganese accumulates as a black oxide coating and biofilm and causes

consumer complaints when it sloughs off during periods of high water usage or change in the water disinfection practice. Such water is aesthetically unacceptable and causes irreversible staining of washing, equipment, manufactured goods and swimming pools.

Manganese and iron related problems have become a significant water quality issue to water supply authorities throughout Australia including South Australia (Thomas, 1985; Cooper, 1989), Victoria (Lowther and Evans, 1980; Earp et al., 1985; Phey and Philips, 1989), the Gold Coast and Pine Rivers Shire of Queensland (Sly, 1987; Sly et al., 1989a) and in the urban regions north and south of Sydney in New South Wales (Ireland, 1986; Waite et al., 1989a). However, it should be recognized that the problem is not unique to Australia with, for example, roughly 40 percent of public water supplies in the United States exceeding recommended levels of iron and/or manganese (AWWA, 1987).

2 RAW WATER QUALITY

2.1 Iron and Manganese in Stored Waters

Manganese and iron problems in many instances have been attributed to the extraction of hypolimnetic waters from thermally stratified reservoirs - particularly in the case of relatively productive waters where sedimenting organic detritus provides an adequate food source for oxygen-consuming organisms. The low oxygen conditions encourage reductive dissolution of iron and manganese oxides present in bottom and suspended sediments with subsequent release to the water column. While Fe(II) so produced may oxidize and reprecipitate relatively quickly on reaching oxygenated waters (depending on pH and extent of organic complexation), the slow rate of oxidation of Mn(II) under such conditions typically ensures maintenance of elevated concentrations of manganese within the hypolimnion for a considerable time. Some idea of the relative rates of (auto)oxidation of Fe(II) and Mn(II) at various pH can be obtained from Figure 2.1. For both iron and manganese, the rates of oxidation of the reduced species (by oxygen) has a squared dependency on the hydroxyl ion concentration [OH^-] however at any given pH, the oxidation rates for Fe(II) and Mn(II) differ markedly. Thus, as can be seen from Figure 2.1, at pH 6.9 the half-time for oxidation of Fe(II) is on the order of minutes while even at pH 9.0, hours are needed before the concentration of manganese is reduced by half.

The residence time of manganese in the water column is dependent on the activity of manganese oxidizing bacteria and on the rate of adsorption onto suspended particles. At pH > 7 the adsorption rate of Mn(II) onto natural suspended solids is greater than its rate of oxidation. The suspended solids consist predominantly of inorganic colloids such as clays and hydrous metal oxides, organic colloidal matter and living microorganisms (Kawashima et al., 1988). At pH 6 to 8 the biological oxidation of Mn(II) to hydrous manganese oxide solids proceeds more rapidly than any non-biological reaction. In waters containing low levels of oxygen, the residence time for Mn(II) undergoing a microbiological conversion to the solid phase has been estimated to be on the order of a few days (Emerson et al., 1982).

Reduced Mn(II) does not bind strongly to either common inorganic ligands or natural organic matter and is typically present in the reduced state as the aquated manganous ion, $Mn^{2+}(aq)$. Only in the presence of high concentrations of organic matter does organic complexation of Mn(II) become significant (Chiswell and Zaw, 1989). Any oxidized

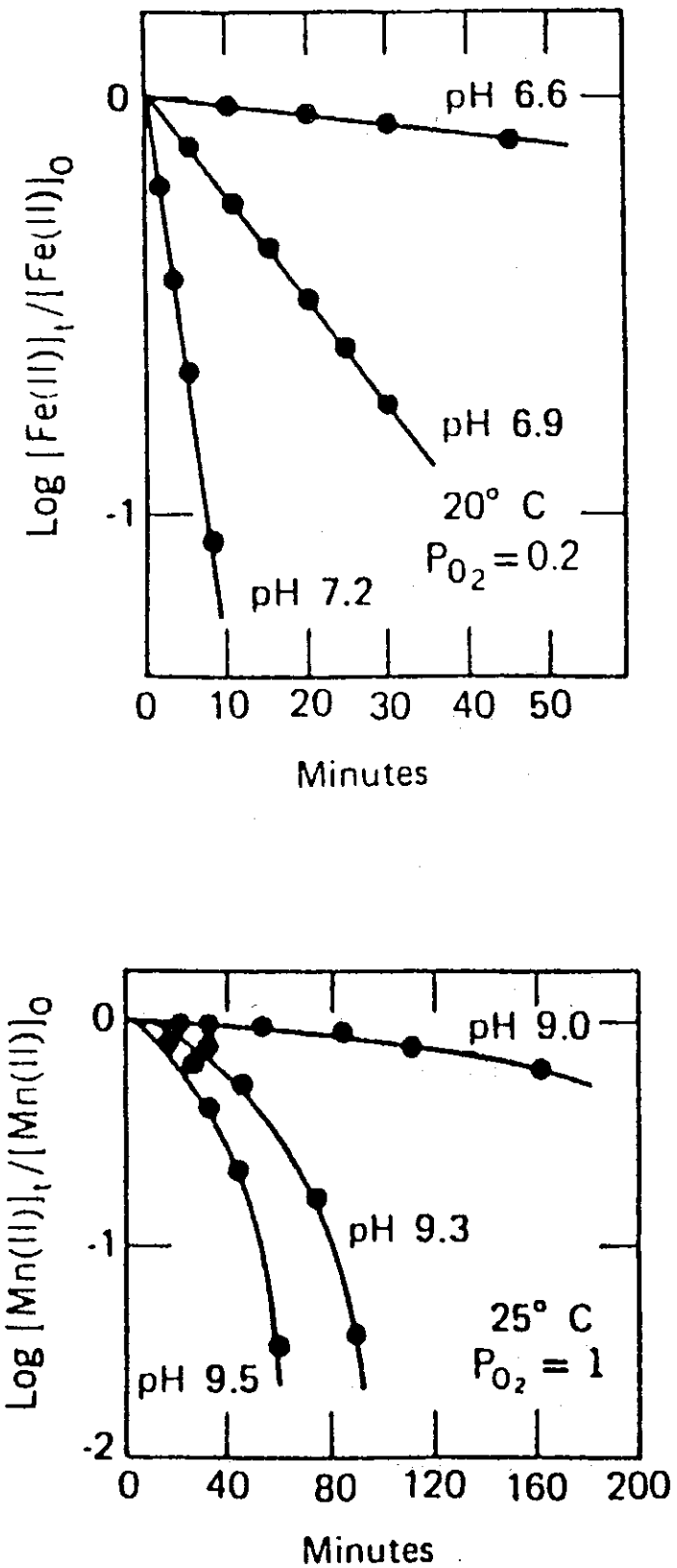

Figure 2.1. Oxidation kinetics of Fe(II) and Mn(II) by oxygen in aqueous solutions (after Stumm and Morgan, 1981).

manganese present will almost certainly be in the particulate Mn(III,IV) oxyhydroxide form since hydrolysis (and subsequently precipitation) readily outcompetes complexation of Mn(III) or Mn(IV) by organic or inorganic ligands.

The situation for iron is a little more complex. Providing the residence time of waters in the reservoir of interest is relatively long (on the order of days) and some oxygen is present, then any Fe(II) should oxidize substantially. The product of oxidation is likely to be a particulate oxyhydroxide (and most likely the amorphous ferrihydrite) though ferric iron interacts strongly with organic ligands (including natural organics such as fulvic and humic acids) and a portion may reside in a soluble, organically bound form (Waite and Morel, 1984). Any iron remaining in the reduced state would most likely be present as Fe^{2+}(aq) or weak Fe(II)-organic complexes or a mixture of both (Waite and Morel, 1984). Of course, organic compounds will have an effect in influencing the aggregation behaviour of both particulate iron and manganese oxides since these negatively charged compounds will adsorb to the oxyhydroxide surfaces. It is to be expected that the adsorption of natural organics to these typically colloidal substances will add stability and lower the tendency for particulate iron and manganese to aggregate and settle out of the water column. Such effects are likely to be of considerable importance in the low ionic strength waters typical of many Australian water supply reservoirs.

The dramatic impact of periodic seasonal thermal stratification of a reservoir on concentrations of dissolved oxygen iron through the water column is clearly seen in results for Cataract Reservoir (south of Sydney) shown in Figures 2.2-2.4. Concentrations of this redox-active element climb dramatically once the hypolimnetic waters become significantly oxygen-depleted. (Similar behaviour is expected for manganese). Further details on the concentration and forms of iron and manganese in impounded waters are provided by Chiswell and coworkers (Chiswell and Zaw, 1989; Chiswell, 1990).

The use of multi-level inlet towers may enable selective extraction of oxygenated epilimnetic waters but such waters, particularly during the summer months, often support high algal populations. In addition, at the onset of winter turnover, high iron and manganese content bottom waters are likely to be mixed with surface waters resulting in a significant reduction in the quality of water entering the treatment plant. Such behaviour following winter turnover is well documented in the results for Mardi Dam, the Wyong Shire water supply reservoir, shown in Table 2.1 (Waite et al., 1989a).

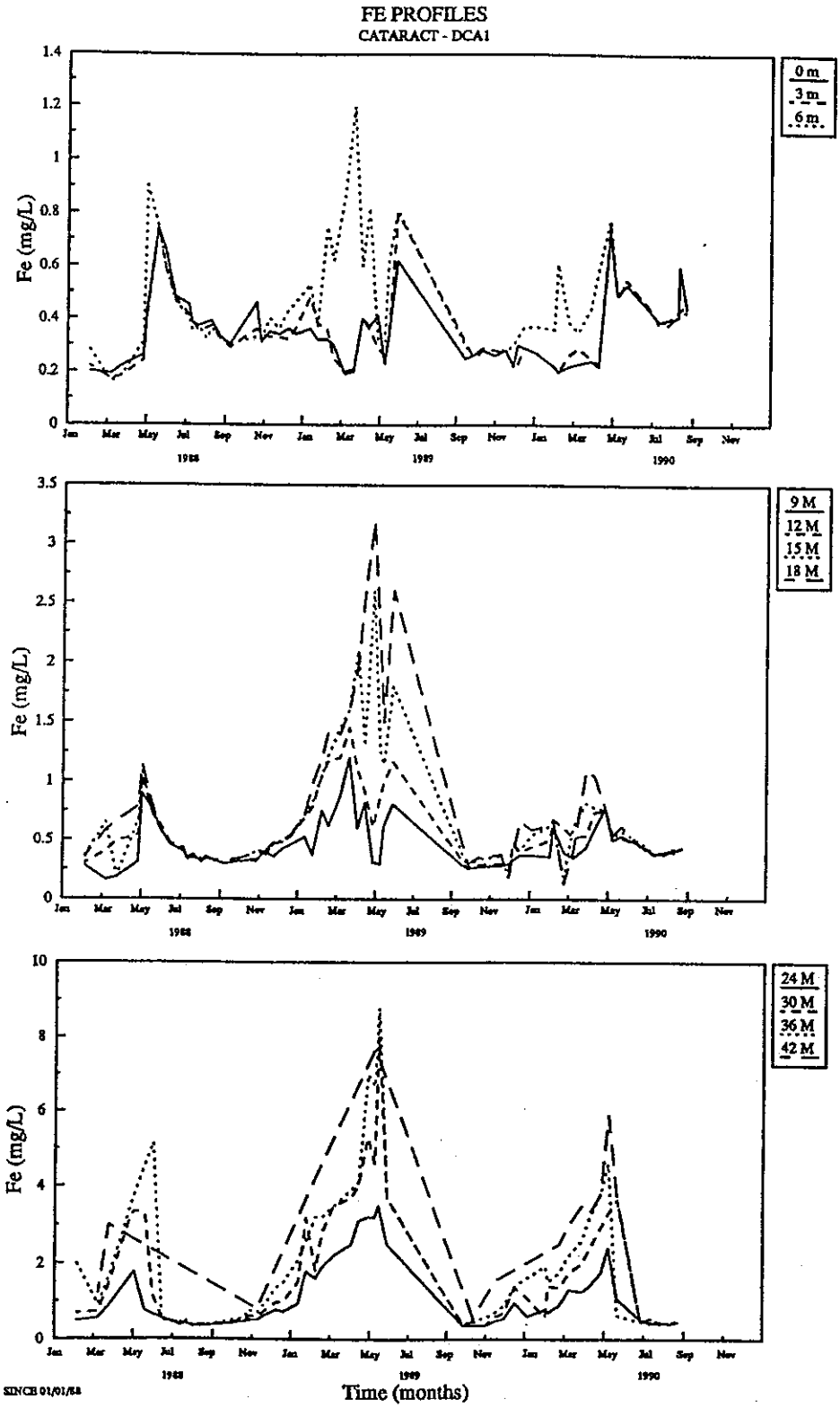

Figure 2.4. Time-series presentation of total iron concentration at various depths in Cataract Reservoir (south of Sydney) over an extended period (Data courtesy of Sydney Water Board).

Table 2.1
Typical values of selected water quality parameters
for near-surface waters of Mardi dam during
summer (stratified) and winter (soon after turnover)

	Summer	Winter
Apparent colour (Hz units)	40	55
Turbidity (NTU)	25	35
Iron ($\mu g\ L^{-1}$)	600	1300
Manganese ($\mu g\ L^{-1}$)	85	200

2.2 Effect of Artificial Aeration on Iron and Manganese

As indicated above, the seasonal thermal stratification of surface water storages can have a profound effect on the quality of water over the depth of the storage. Artificial destratification is the process of adding energy to a water body to break down existing stratification, or more usually, to prevent the onset of stratification. By artificially preventing stratification, oxygen supply to the bottom waters of a storage can be maintained and thus prevent the release of iron and manganese from the sediments.

Aeration/destratification is a management technique which has been widely used internationally (Raman and Arbuckle, 1989) and in Australia (Brown,1986; Chiswell and Zaw, 1990) to effect beneficial changes in the thermal, chemical and biochemical status of both man-made and naturally occurring water storages. The method is now recognized as an effective way of minimizing the release of iron and manganese from sediments and is being used increasingly in Australian reservoirs for water quality improvement purposes (Loos, 1987). Oxygen saturations maintained at above 5% throughout the water column are claimed to be sufficient to prevent high concentrations of iron and manganese developing (Bowles et al., 1979). Two additional benefits of the introduction of artificial destratification are the maintenance of uniform water quality within the reservoir throughout the year, and the maintenance of maximum residence time of water within the reservoir. Sufficient residence time is required to ensure complete formation of particulate forms of iron and manganese which may subsequently sediment out of the water column (Waite et al., 1989b).

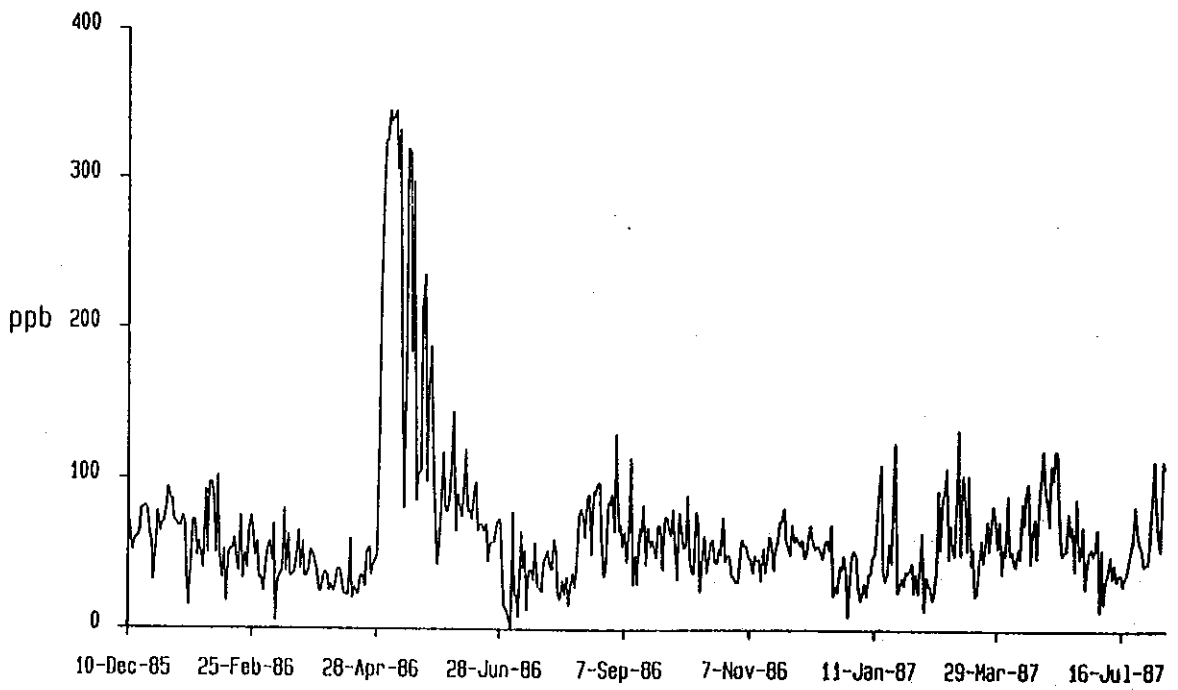

Figure 2.3. Concentration of total manganese in raw waters from Mardi Dam entering the Wyong Shire water treatment plant. Values determined using the persulphate colorimetric method.

3 TREATMENT OPTIONS FOR IRON AND MANGANESE REMOVAL

3.1 Overview

Obviously, it is not always possible to ensure that iron and manganese concentrations in raw waters are below the levels recommended for drinking waters and, in such instances, removal methods must be implemented within the treatment plant. Common methods of treatment involve the oxidation of soluble Fe(II) and Mn(II) to insoluble Fe(III) and Mn(III,IV) using relatively powerful oxidants such as chlorine, chlorine dioxide, potassium permanganate or ozone. Oxidation is then followed typically by removal of the iron and manganese precipitates by filtration, sometimes preceded by flocculation and, in some instances, sedimentation. Another treatment technique is to sequester Fe and Mn by the nearly simultaneous addition of sodium silicate and chlorine (Robinson et al., 1987; Robinson and Ronk, 1988) or by the addition of polyphosphates. Other treatment methods include ion exchange and the use of special filter media such as manganese greensand that catalyzes oxidation and removal.

In Australia, oxidation-precipitation-filtration treatment procedures are used in the majority of cases and most of the ensuing discussion focusses on such systems. The alternative methods presented above are being used increasingly widely in Europe and North America, especially by small water systems (AWWA, 1987; Viraraghavan et al., 1987), but have been used only sporadically here. For example, silicate addition has been successfully used for iron stabilization in the Wagga Wagga region in New South Wales (Baker, 1986) and a manganese greensand system has been implemented at the Petrie Water Treatment Plant in the Pine Rivers Shire in Queensland.

In most Australian treatment plants in which some method of iron and manganese control is implemented, the raw waters entering the plant are monitored at regular intervals (and in some cases continuously) for iron and manganese concentrations. Type and quantity of oxidant used is typically determined by the levels observed. In most cases, colorimetric methods of analysis are used with the phenanthroline method for iron (APHA Method 315A; APHA, 1980) and the persulphate method for manganese (APHA Method 319B; APHA, 1980) most common. It should be noted that the currently adopted standard colorimetric methods, particularly for manganese, may lead to significant overestimation of concentrations present and caution in data interpretation must be exercised. Improved colorimetric methods for manganese (such as the porphyrin method) (Ishii et al., 1982; Aldridge et al., 1989) and relatively inexpensive atomic absorption instruments

are now available and consideration should be given to their use by water authorities concerned with iron and manganese. Additionally, the water treatment method adopted will be dependent on the form of the element present and analytical techniques that provide information on chemical speciation must be adopted.

3.2 Oxidation

As discussed above, both iron and manganese may be present in source waters in their soluble +II oxidation states and, as such, require an oxidation step to bring them to a particulate (more easily removable) form. Ferrous iron is relatively easy to oxidise and does so relatively rapidly in the presence of mild oxidizing agents (oxygen, chlorine) at pH's over 7 (the autooxidation rate exhibits a squared dependency on hydroxyl ion concentration). However, pH's > 10 are required for the oxygen induced oxidation of Mn(II) to occur at timescales short enough to be of interest. Such pH increases are not feasible in the treatment plant. Rather, it is typical that more powerful oxidants are added to speed up the oxidation step.

Four reagents have been commercially used for the oxidation of dissolved Mn(II) to particulate oxide form prior to removal via coagulation and filtration, namely, chlorine, potassium permanganate, chlorine dioxide and ozone. The standard potentials of these oxidants, are as follows (Weast, 1977):

$$O_3 + 2H^+ + e^- = O_2 + H_2O \qquad 2.07\ V$$

$$MnO_4^- + 4H^+ + 3e^- = MnO_2 + 2H_2O \qquad 1.68\ V$$

$$ClO_2 + H^+ + e^- = HCLO_2 \qquad 1.27\ V$$

$$HClO^- + H^+ + 2e^- = Cl^- + H_2O \qquad 1.49\ V$$

Comparison of the standard potentials of these redox processes with those of the iron and manganese redox reactions of interest; i.e.

$$MnO_2(s) + 4H^+ + 2e^- = Mn^{2+} + 2H_2O \qquad 1.23\ V$$

$$Fe(OH)_3(am) + 3H^+ + e^- = Fe^{2+} + 3H_2O \qquad 0.95\ V$$

indicates that each of these oxidants should indeed induce the formation of the solid manganese and iron oxyhydroxides (interestingly, and as indicated by the redox potentials given above, ozone can induce the further oxidation of MnO_2 to soluble permanganate). A

more quantitative estimate of the driving force for these redox processes requires more careful analysis of these processes under the conditions (particularly of pH and reactant concentrations) of interest.

In addition to the oxidation of Fe(II) and Mn(II) (if present), the addition of oxidants such as ozone, chlorine and potassium permanganate will also induce the oxidation of organic compounds present in the source waters. Such oxidation is likely to be only partial (i.e. not proceed completely to CO_2 and H_2O) and may:

- result in an increase in the effectiveness of the coagulation and filtration processes.
- result in the formation of troublesome organic compounds. For example, the ozonation process produces easily assimilable low-molecular-weight organic compounds (AOC) which can enhance regrowth of microorganisms in the water reticulation system. Likewise, the chlorination process causes the formation of halogenated organic compounds which are sometimes referred to as total halogenated methane compounds (THM) or adsorbable organic halogen (TOX) (Kruithof *et al.*, 1989). The health implications of the use of such oxidants are discussed further in Section 3.2.5.

More detailed discussion of the positive and negative aspects of the use of these reagents for iron and manganese removal is given below.

3.2.1 Chlorine

Chlorine (through the active oxidizing agent, hypochlorous acid) is effective in enhancing the oxidation of ferrous iron to easily removable particulate form but the soluble manganous ion is much more resistant to chlorine-induced oxidation. The rate of oxidation of Mn(II) by chlorine (NaOCl) at different pH values is shown in Figure 3.1 and indicates that even at pH 8.5 the oxidation process still takes 40 minutes to come to completion (Khoe and Waite, 1989). Given that Australian raw waters are typically in the neutral to slightly acidic pH range, extended (and typically unreasonably long) contact times within the treatment plant prior to the final filtration step are needed to ensure complete oxidation of any Mn(II) present if chlorine is used for this task. The odour problems associated with excessive chlorine dosing and the increasing concern over the formation of trihalomethanes through pre-chlorination of raw waters high in organic content also mitigate against the use of this oxidant.

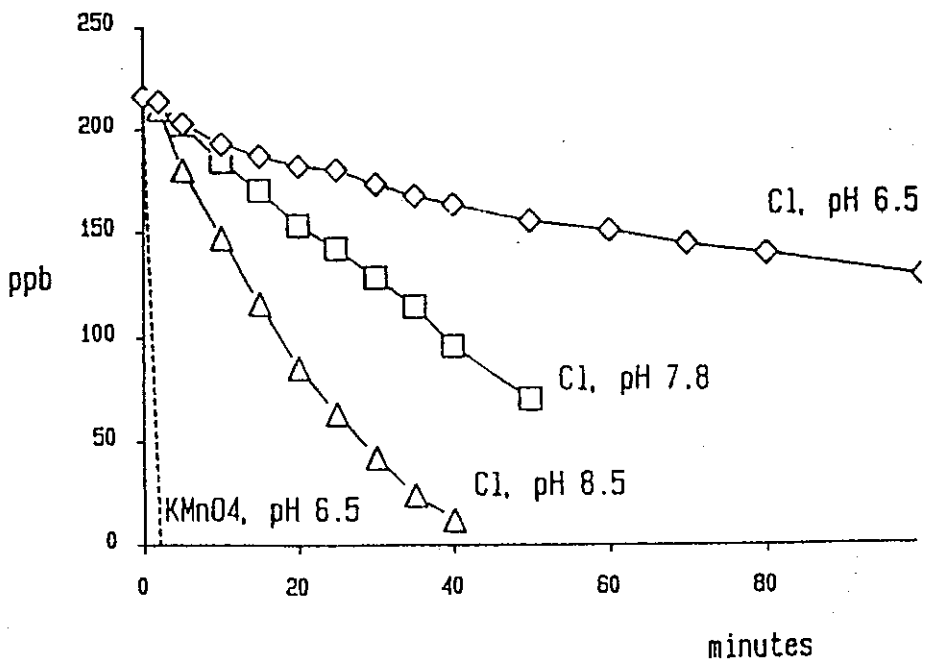

Figure 3.1. Oxidation of manganous ion by excess hypochlorous acid at various pH. For comparative purposes, the oxidation of Mn^{2+} by excesss potassium permanganate is also shown.

The lack of effectiveness of chlorine in the oxidation of Mn(II) is exemplified through results obtained at the Wyong Shire water treatment plant. The results of analyses for filterable (<0.22 μm) manganese concentrations in raw, flocculated and filtered flocculated-water at this plant are shown in Figure 3.2. The input water was chlorinated before the addition of alum and polyelectrolyte. It appears that there was not enough time for significant chlorine-induced oxidation to occur with a resultant inability of the alum flocs to scavenge the filterable manganese. The assumption that the < 0.22 μm fraction of manganese is dissolved rather than fine colloidal appears most consistent with the available data (15). In contrast to manganese, the filterable (< 0.22 μm) iron in the dam water was efficiently removed by the flocculation process (Figure 3.3). It is presumed that the filterable (< 0.22 μm) iron fraction had already been oxidised to the particulate ferric state (either in the dam or in the pre-chlorination step) by the time of alum addition.

Wong (1984) documented similar findings using chlorination followed by dual media (anthracite-sand) filtration. It was shown that prechlorination is effective in oxidising manganese if a pH of greater than 8.5 is maintained. It was also reported that there was a dramatic difference between the use of NaOH and $Ca(OH)_2$ as the pH-correcting agent. When the latter was used, manganese levels in the filter effluent were reduced from 2 mg L^{-1} to below 0.05 mg L^{-1}. The effectiveness of manganese removal has been attributed to the neutralisation of surface charge by the specific adsorption of Ca^{2+} ions. The fact that MnO_2 adsorbs Ca^{2+} (and other cations such as Mg^{2+} and Zn^{2+}) is well documented. Posselt et al. (1968) and Jenkins and Engeset (1975) have shown that Ca^{2+} uptake does reduce the net charge of colloidal MnO_2 and that this reduction in charge leads in turn to destabilisation of the colloid. They also observed that monovalent ions such as Na^+ had no significant influence on the coagulation of MnO_2 within the range of concentrations of interest. Similar effects of Ca^{2+} addition have been reported by Jenkins et al. (1984).

The use of chlorine as the preferred oxidant for Mn(II) has also been reported by Bratby (1988) for a water treatment plant in Brazil. In this case, because the optimal pH for manganese removal (pH > 8.5-9.0) was so much higher than the optimal pH for colour and turbidity removal (near neutral pH), the pH was raised through lime addition **after** addition of coagulant ($FeCl_3$). In this way, effective removal of colour and turbidity was achieved at the lower pH while efficient oxidation and aggregation of

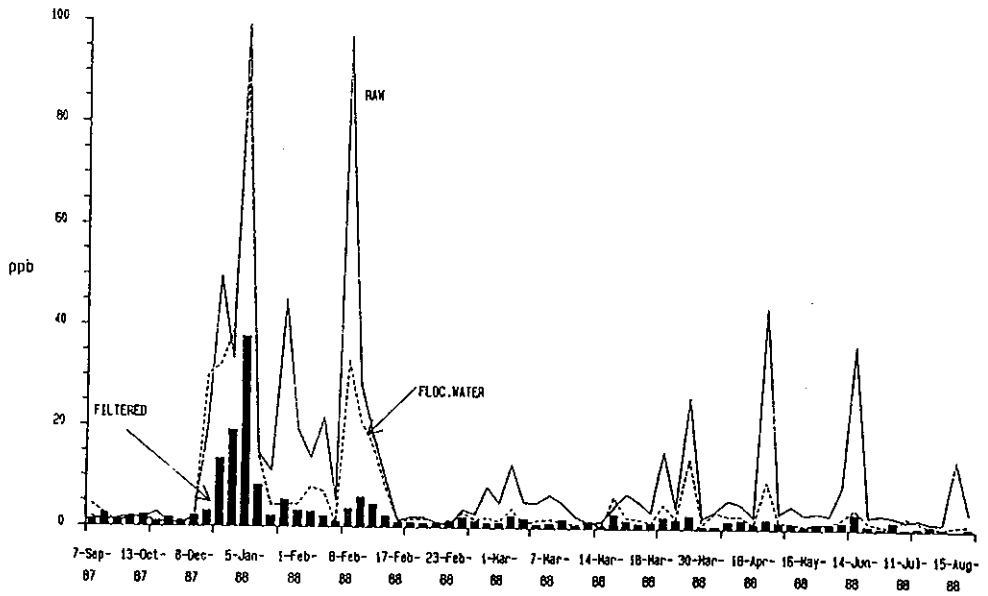

Figure 3.2. Filterable (<0.22 μm) manganese concentrations in raw waters, waters from the filter inlet channel (after coagulant and coagulant aid addition) and filtered waters from Wyong Shire water treatment plant.

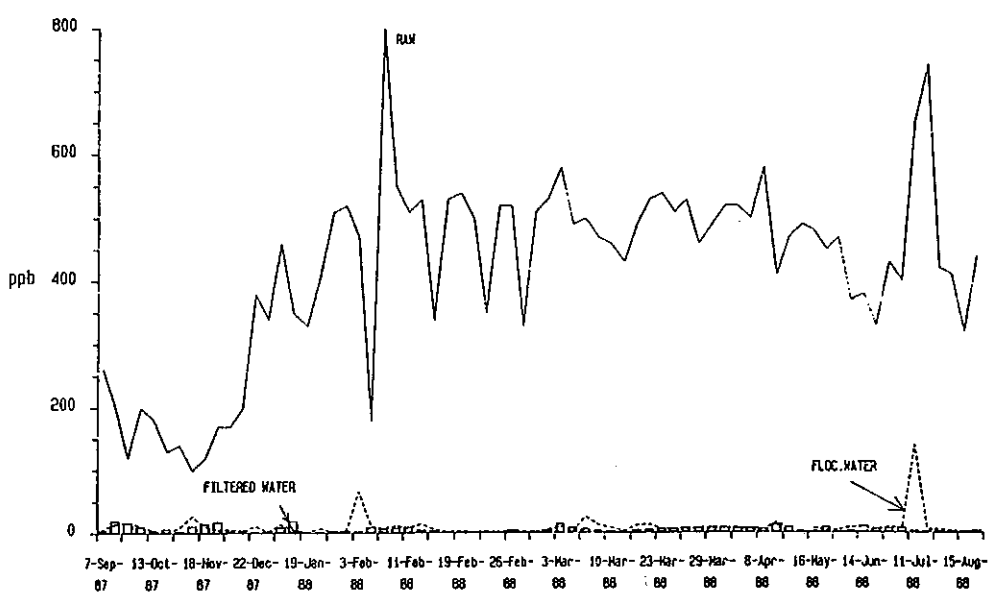

Figure 3.3. Filterable (<0.22 μm) iron concentrations in raw waters, waters from the filter inlet channel and filtered waters from Wyong Shire water treatment plant.

manganese was achieved at the higher pH. Presumably, the rate of desorption of organic and particulate contaminants (i.e. those contributing to colour and turbidity problems) from the iron oxide flocs at the higher pH was relatively slow.

3.2.2 Potassium permanganate

Potassium permanganate has long been recognised as an effective reagent for oxidation of a broad range of impurities commonly found in natural waters. It now has wide acceptance in water treatment practice for taste and odour control and the oxidation and subsequent removal of reduced forms of iron and manganese (Ficek, 1978; Loos, 1987).

Based on reaction stoichiometry; i.e.

$$3Mn^{2+} + 2MnO_4^- + 2H_2O \rightarrow 5MnO_2 + 4H^+$$

$$3Fe^{2+} + MnO_4^- + 7H_2O \rightarrow 3Fe(OH)_3 + MnO_2 + 5H^+$$

1.92 mg $KMnO_4$ is required to oxidize 1 mg of Mn^{2+} and 0.94 mg $KMnO_4$ will oxidise 1 mg of Fe^{2+}. In actual practice, the required amount of potassium permanganate dose is normally less than the stoichiometrically predicted amount because of the ability of the freshly formed oxyhydroxides to heterogeneously catalyse further oxidation. Potassium permanganate is also effective in rapidly oxidizing many naturally occurring organic compounds thus an excess over the stoichiometric amount required to oxidize the manganous ion in raw water must be used. Indeed, Knocke *et al.* (1987) found that when the TOC was <3 mg L^{-1}, the required permanganate dosage was typically less than 10-20% above the stoichiometric requirement (1.92 mg of $KMnO_4$ per mg of Mn^{2+}). When the TOC was 8 mg L^{-1} essentially no manganese oxidation was observed until nearly 1.5 mg L^{-1} of permanganate was added. 1.5 mg/L of permanganate were required to oxidize 8 mg/L TOC before any significant manganese oxidation occurred.

In comparison with Mn(II) oxidation by oxygen or chlorine, the rate of oxidation of Mn(II) by permanganate is rapid. The rate of the redox process is pH dependent and decreases on decreasing the pH. At pH 5 and 2 mg/L of Mn^{2+} and MnO_4^-, complete oxidation is observed after about 10 minutes. The required reaction time at pH 6 is approximately complete in about half this time (Ficek, 1978; see also Figure 3.1). Reaction rates with organic compounds are significantly slower than with Mn^{2+}. For example, Colthurst and Singer (1982) studied the rate of oxidation of aquatic

fulvic acid (1.9 mg L^{-1}) by an excess concentration of $KMnO_4$ (8.0 mg L^{-1}). About 1 mg L^{-1} of $KMnO_4$ was consumed in 50 minutes - a rate significantly slower than expected for the oxidation of Mn(II) under equivalent conditions.

Concern over "overdosing" of potassium permanganate has been expressed by some water treatment plant operators with the resultant production of "pink" water. This concern highlights the need for more detailed information on the conjunctive demands for permanganate by raw water constituents. In addition, relatively simple "residual" potassium permanganate monitors based on the electrochemical detection of permanganate are now available and consideration should be given by the water authorities to their purchase or construction for the purpose of dose control (possibly in a feedback mode).

3.2.3 Chlorine dioxide

ClO_2 is a greenish-yellow gas which is soluble in water (0.3-1%). It is volatile and can be easily stripped from solution by vigorous aeration. The ClO_2 vapour will explode under the slightest shock (eg water hammer) if it is present at concentrations greater than 10%. Because it is sensitive to temperature and pressure it cannot be shipped in bulk and must be generated on site. One method of generation is from the reaction of $NaClO_2$ solution and chlorine. ClO_2 decays within six hours to form ClO_2^- (48%), ClO_3^- (22%) and Cl^- (28%). The measurement of the residual ions is difficult. There are as yet no test kits for chlorine dioxide. In addition, an excessive level of chlorine dioxide in potable water has an adverse health effect which is similar to that of nitrate. The USEPA limits the total concentration of ClO_2, ClO_2^- and ClO_3^- present in potable water to < 1.0 mg L^{-1} (Pascoe and Loos, 1990).

The following advantages of ClO_2 have been documented by Pascoe and Loos(1990):

- aids coagulation;
- does not form THM's and forms less TOX (total organic halides) than Cl_2. It reduces the formation of THMs by any subsequent chlorination;
- effective disinfectant (even against Giardia cysts);
- oxidises tastes and odour compounds better than Cl_2;
- produces less aldehydes and ketones than O_3 and is currently about one-quarter the cost of O_3;

- a number of companies in Australia can offer reliable equipment for ClO_2 dosing.

Carlson *et al.* (1987), however, showed that ClO_2, as a preoxidant by itself, is not effective in removing Mn(II) when the TOC in the water is ≥ 5 mg L^{-1} (at pH 6.3). In water with significant TOC levels, permanganate can be used in conjunction with ClO_2 to oxidise Mn(II) without forming THM's. However, chlorine dioxide causes permanganate to persist in the Mn(VII) state, even at low pH (6.3) and a high TOC concentration (5 mg L^{-1}). Permanganate alone was found effective for oxidising Mn(II) even with TOC at 5 mg L^{-1} and at pH 6.3. Knocke *et al.*(1987) reached the same conclusion concerning the use of ClO_2 as a preoxidant for manganese. But their reason for the unsuitability of ClO_2 for high TOC waters was the regulatory limits for ClO_2 dosage (in USA 0.5-2.0 mg L^{-1} because of health concerns related to the presence of chlorite and chlorate in water).

3.2.4 Ozone

Ozone has been used extensively in the oxidative removal of iron and manganese from groundwaters. A number of case specifife examples are given below:

- Weissenhorn (1984) reported on the use of ozone for iron and manganese removal in a water treatment plant in Dusseldorf, Switzerland. The removal of up to 0.5 mg L^{-1} manganese and 0.1 mg L^{-1} iron is effected with the use of ozone at a concentration of 1.5 to 2.5 mg L^{-1}, depending on the raw water quality, followed by filtration through a bed of granular activated carbon (GAC) and sand filter. Apart from the removal of particulate matter and the AOX, the GAC filter also reduces permanganate ions (produced by excess ozone) to insoluble manganese dioxide.
- Stoebner and Rollag (1985) used ozone to treat a municipal ground water supply at Brookings, South Dakota in order to reduce iron, manganese and THM formation. The ground water has iron concentrations in the range 4 to 5 mg L^{-1} and manganese in the range of 0.6 to 0.7 mg L^{-1}. The total THM concentration in the $KMnO_4$ treated, filtered and chlorinated water was normally 32 ppb. It was found that at ozone dosages of 2 mg L^{-1} or greater and a detention time of ≥5 min, essentially all of the iron was oxidised. For manganese, the required dosage, at 5 min detention time or greater, was 4 mg L^{-1}. Increasing the ozone dosage above 4 mg L^{-1} did not improve the extent of iron and manganese oxidation. In fact, the use of ozone dosages > 4 mg L^{-1} produced pinkish water due to the oxidation of manganese to permanganate.

Stoebner and Rollag (1985) further found that ozone-formed iron and manganese flocs are more difficult to filter (using anthracite filter) than are oxygen-formed flocs. They recommended the use of fine sand (20 mesh) filter to remove the ozone-oxidised particles. Total THM's produced was reduced from 26 to 15 ppb by ozonation.

- In a study on the effect of ozonation on the removal of iron from a ground water, Cromley and O'Connor (1985) investigated the effectiveness of ozone in alleviating the problem of interference by organics in the water. Organic compounds interfere in the removal of iron from ground water by peptizing the ferric hydroxide flocs, forming complexes with ferric ions, or by reducing ferric ion to ferrous. They found that ozonation resulted in more rapid oxidation of ferrous ions than aeration. Furthermore, it resulted in the destruction of some but not all of the TOC. They found that, given unlimited reaction time (> 30 minutes), aeration of the water actually gave better removal of iron than in the case of treatment with ozone. They hypothesized that the incomplete destruction of the TOC by ozone actually enhanced the extent of organic interference of the residual organics by increasing the number of carboxylic functional groups. This led to an increase in the extent of formation of soluble ferric-carboxylate complexes.

The question of effect of ozonation on the removal of iron and manganese from surface waters has also been addressed by some authors. For example;

- Yapijakis (1986) has shown that high quality water for small communities can be obtained by using a process consisting of ozonation followed by diatomaceous earth filtration. However, it was considered that the particulate ferric oxide resulting from ferrous iron oxidation was more gelatinous than produced by air oxidation with a resultant reduction in filter run times due to increased tendency of the filter to block.
- Weng et al. (1986) report on a five year pilot plant study in New Jersey in which coagulation, ozonation and direct filtration were used to produce a finished water of high quality. It was concluded that use of ozone would reduce the amount of alum needed thus reducing the amount of sludge produced. Despite the addition of ozone, a significant portion of the soluble, reduced manganese present in the source waters passed through the plant and was removed (with varying degrees of

success) by the depth filters. Ageing of the filters was found to improve the removal efficiency as was continual regeneration of the manganese oxide coating through application of a slight residual of chlorine at the filter.

The results of a number of bench-scale studies aimed at clarifying the nature of the interactions and processes operating in these complex systems have also been reported in the literature. For example:

- Chédal (1984) reported that the solution pH required for metal hydroxide precipitation is reduced by the use of ozone. This is caused by the increase in the oxidation potential of the solution as a result of ozonation. Furthermore, ozone can break down the metal-organic complexes which also leads to the elimination of these metals from solution. The latter was demonstrated by the action of ozone on EDTA-Mn complexes: the manganese concentration in the solution was reduced (precipitated and removed from solution) from 2750 ppb to 275 ppb in ten minutes with an ozone concentration of 1 mg L^{-1}.
- The kinetics of oxidation of iron(II) and manganese(II) by ozone has been studied by Abukhudair *et al.*(1989) and observed to follow zero order kinetics. The reaction rate constant for iron(II) at pH 6 and an ozone dosage of 1.96 mg L^{-1} and initial iron(II) concentrations of 4, 3, 2, 1 mg L^{-1} are 0.49, 0.41, 0.372 and 0.352 mg $L^{-1}min^{-1}$ (the rate constant is reported to decrease with the increase in ozone dosage per initial concentration of ferrous ions; further research work is warranted to confirm this). The rate constant for manganese(II) at initial Mn(II) of 4 mg L^{-1}, ozone dosage of 1.96 mg L^{-1}, and pH values of 6 and 7 are: 0.29 and 0.31 mg L^{-1} min^{-1}. If the order of the oxidation reaction is zero as reported here, then the detention time required is proportional to the initial iron(II) and manganese(II) concentrations.
- Paillard *et al.* (1989) investigated the removal of iron and manganese with ozonation in the presence of humic substances. The studies were carried out using synthetic water, with and without the spiking of humic material, and raw water obtained from the Moulin-Papon (France) dam. They found that while iron was easily removed (even without an oxidation step), ozonation (1 mg L^{-1}) at a pH of nearly 8.4 did not succesfully remove manganese unless a significant amount of alkalinity (120 to 130 mg L^{-1} as $CaCO_3$) was added before the

oxidation-coagulation-filtration stage. The presence of humic substances was also found to increase the ozone dosage required to well above the stoichiometric level (0.87 g O_3/g Mn^{2+}).

Some insight into the role of alkalinity in the removal of manganese can be gained by considering the oxidation process in more detail. The oxidation reaction of ozone can occur via two different pathways (Staehelin and Hoigne, 1985):

(i) A direct oxidation reaction by molecular ozone. Ozone molecules react with specific sites of organic compounds containing aromatic, unsaturated aliphatic or nitrogen groups;

(ii) An indirect oxidation reaction by radical species (such as $OH^{\cdot}$, $O_2^{\cdot -}$, $HO_2^{\cdot}$) produced by the decomposition of ozone in water. The production of these radical species is enhanced at high pH (i.e. high [OH^-]).

In most cases, these two reaction pathways coexist, their relative contributions depending on the characteristics of the water. The oxidation of manganese is favoured by the second reaction pathway. Thus, manganese oxidation will be favoured over the oxidation of organic materials under solution conditions favouring the second pathway. The pH increase that would presumably accompany an alkalinity increase should thus lead to an enhancement in oxidation of Mn(II) (Paillard *et al.*, 1989a).

In addition to the effect of increase in pH, the added calcium ions present (if lime is used) should improve the aggregation and flocculation of the colloidal manganese oxides produced in the oxidation step.

3.2.5 Adverse effects of oxidant use

Although the oxidants themselves do not pose risks of adverse health effects at the concentration levels commonly found in the treated waters, concerns have been reported regarding the health effects of their by-products. These can be present as modified oxidant molecules or partially oxidised organic substances.

Kruithof *et al.* (1989) investigated the effects of ozonation on humic substances in water. Ozonation converts humic material to low-molecular-weight biodegradable compounds which are more easily assimilated by microorganisms. If these are not removed, they can promote microbial infestation in the reticulation system. Other

residuals produced by ozonation which may have toxicological significance are aldehydes. However, the health effects significance of these compounds has not been determined (US EPA, 1989).

The reaction of chlorine with organic substances produces three major groups of chlorination by-products: trihalomethanes, chlorinated acetic acids, and haloacetonitriles. To date, three THMs have been implicated as carcinogens in animals: chloroform, chlorodibromomethane, and bromodichloromethane (US EPA, 1989).

The use of pure chlorine dioxide for primary disinfection and manganese oxidation purposes does not form THMs. However, its use is complicated by the toxicological effects of the by-products, chlorite and chlorate which produce methemoglobinemia (as in cases of poisoning by nitrites) (US EPA, 1989). The limit recommended by the US National Research Council was 0.21 mg L^{-1}. However, a recent report produced by the Office of Drinking Water USEPA stated that this figure should be modified to 0.06 mg L^{-1} in order to take into account children's higher sensitivity to oxidants than adults (US EPA, 1989).

3.3 Coagulation/Flocculation

As implied above, in addition to the requirement for oxidation of Mn(II) and Fe(II) to insoluble particulate species, the oxides so formed must be large enough to either sediment efficiently or, in the absence of a sedimentation stage, be trapped on the filter media being used. The susceptibility of the oxide particles to aggregate will be particularly dependent upon net surface charge - a characteristic that is very dependent on the nature of the particles, the presence of specifically adsorbed species (such as natural organic compounds) and solution conditions and which may be manipulated typically through the addition of coagulants and coagulant aids. For example, over the pH range of practical interest for water treatment operations ($5 < pH < 11$), manganese oxides produced either by bacterial or permanganate-induced oxidation exhibit a net negative surface charge and are thus susceptible to destabilization by cationic additives. The pH at which the surface charge is zero (pH_{pzc}) is around 2-3 for manganese oxides and 7-9 for iron oxides. Thus, in most instances, at the pH typically used in most water treatment plants (6-9), iron oxides are expected to possess low surface charge compared to manganese oxides and thus aggregate more readily.

As outlined in Chapter 1, two approaches to investigation of aggregation processes have been adopted here:

- investigation of optimal treatment plant conditions for aggregation of manganese oxides has been undertaken using waters from the Wyong Shire's Mardi Dam. (Particular attention has been given in these studies to manganese rather than iron removal because of the ease of removal of iron from these waters). Selected results of these studies are discussed below. Further details of these studies may be found elsewhere (Waite et al., 1989a).
- fundamental studies of the factors controlling rate of aggregation and size of aggregated oxides. While preliminary aggregation studies were conducted on manganese oxides (Stubbings et al., 1987), the most useful results were obtained on iron oxides of relatively well defined morphology. The results of these studies are reported in some detail in Appendix 1. As indicated in Appendix 1, our ability to describe the dependency of aggregate size on solution conditions for relatively simple systems is adequate but considerably more work is required in understanding the interactions in more complex systems typical of the water treatment plant.

3.3.1 Choice of coagulant and coagulant aid

Alum is the most common coagulant used in Australian water treatment plants and appears to be an effective agent for assistance of the aggregation of manganese oxides - most likely through interaction of polycationic aluminium hydroxy species with the negatively charged manganese particles (Posselt *et al.*, 1968). Polymerised aluminium coagulants (such as polyaluminium chloride, PAC) have also been used extensively in the US and are attractive because of the significant reduction in amount of Al-containing sludge produced but their use has been limited in Australia. Given the continuing documentation of relationships between the presence of aluminium in drinking waters and the incidence of Alzheimer's disease (Martyn et al., 1989) and the relatively narrow optimal pH operating range for aluminium coagulants, increasing consideration is being given to the use of ferric-based coagulants. In addition, some consideration for the purpose of iron and (particularly) manganese removal has been given to liquid cationic coagulants such as Superfloc C573 (a low molecular weight polyamine marketed by Cyanimid) and Ultrion (produced by Nalco and marketed by Catoleum).

During the course of this study, investigations of the type and quantity of coagulant and coagulant aid required to optimize manganese and colour removal from Mardi Dam waters were undertaken. Samples of Mardi Dam water which had been stored in oxygen-impermeable bags at 4°C were used for these laboratory investigations. As

indicated in Table 3.1, these waters were of low turbidity. These waters were also of low hardness (ca. 25 mg $CaCO_3$/L) and low alkalinity (ca. 16 mg $CaCO_3$/L). Given the relatively low concentration of manganese in these samples, dissolved manganese (as $MnCl_2$) was added in some instances. Potassium permanganate was also typically added 15 minutes prior to alum dosing ensuring complete formation of oxidized, particulate manganese. In all cases, the sample was stirred (125 rpm) for one minute after addition of chemical oxidant, left standing for about five minutes, dosed with coagulant and coagulant aid (flocculant), stirred (125 rpm) again for one minute, and slowly stirred (at 25 rpm) for 20 minutes before being filtered using memebranes of 3 micron pore size.

Studies were initiated with alum and the flocculant LT20 - the chemicals recommended at the design stage and used routinely in the treatment process. The experimental results shown in Table 3.1 indicate that an alum dose of 10 mg/L and a polymer (LT20) dose of 0.1 mg/L are the minimum concentrations required to ensure formation of good sized flocs in 20 minutes or less (the residence time in the cell above the sand filter is estimated to be < ca. 20 minutes). While it is recognized that the optimum alum dose with respect to filter run time may be less than 10 mg/L, these dosages have been used in most of the work reported here.

The addition of both non-ionic and cationic polymeric coagulant aids (LT20 - nonionic; LT22, LT24 - cationic) was found to increase the size of flocs with 2 mm and 4mm flocs formed in the absence and presence of polymers respectively but does not appear to significantly improve manganese or colour removal. A slight increase in the manganese removal efficiency (from 85% to 90%) was observed on increasing calcium concentration from 5 to 40 mg/L. Similar increases in manganese removal efficiency with increased Ca^{2+} concentration have previously been reported (Jenkins et al., 1984) and presumably reflect the ability of the divalent calcium ion to destabilize the negatively-charged manganese oxide particles.

More significant effects are observed on altering the primary coagulant. The manganese removal efficiencies with the liquid cationic coagulants Ultrion and Superfloc C573 are compared with those obtained using alum in Table 3.2. Best results are obtained using Ultrion at an uneconomical concentration of 16 mg/L followed by alum (10 mg/L) + LT20 (0.1 mg/L). (Note that the dosage of alum is expressed as mg of alum salt per L while that for Ultrion is mg of liquid per L). Doubling the alum dose to 20 mg/L does not increase its manganese removal capability.

Raw Water		Alum Dose	LT20 Dose	Rapid Mix		Flocculation		
pH	Turb,NTU	mg/L	mg/L	rpm	sec	rpm	min	Floc Size
6.95	0.7	2	0.1	125	80	25	20	nil
6.95	0.7	6	0.1	125	80	25	20	nil
6.95	0.7	10	0.1	125	80	25	20	E (2 mm)
6.95	0.7	14	0.1	125	80	25	20	F (3 mm)
6.95	0.7	18	0.1	125	80	25	20	G (4 mm)
6.95	0.7	22	0.1	125	80	25	20	G (4 mm)
6.92	0.6	8	0.1	125	80	25	20	A (0.5 mm)
6.92	0.6	10	0.1	125	80	25	20	F (3 mm)
6.92	0.6	12	0.1	125	80	25	20	G (4 mm)
6.92	0.6	14	0.1	125	80	25	20	G (4 mm)
6.92	0.4	8	0.2	125	80	25	20	B (0.8 mm)
6.92	0.4	10	0.2	125	80	25	20	F (3 mm)
6.92	0.4	12	0.2	125	80	25	20	F (3 mm)
6.92	0.4	14	0.2	125	80	25	20	G (4 mm)
6.92	0.4	8	0.02	125	80	25	20	A (0.5 mm)
6.92	0.4	10	0.02	125	80	25	20	C (1 mm)
6.92	0.4	12	0.02	125	80	25	20	E (2 mm)
6.92	0.4	14	0.02	125	80	25	20	F (4 mm)
6.86	0.4	8	0.05	125	80	25	20	A (0.5 mm)
6.86	0.4	10	0.05	125	80	25	20	C (1 mm)
6.86	0.4	12	0.05	125	80	25	20	E (1 mm)
6.86	0.4	14	0.05	125	80	25	20	F (4 mm)

The turbidity in the flocculated and filtered (2.5 μm) water was about 0.2 NTU (nephelometric turbidity unit).
LT20 is a Magnafloc non-ionic flocculant

Table 3.1. Results from preliminary flocculation experiments on raw waters from Mardi Dam using various doses of alum and Magnafloc LT20.

Table 3.2. Effect of different coagulants and coagulant/flocculant combinations on floc size and efficiency of removal of manganese and colour from Mardi Dam waters.

Mn-spiked Water			Added Chemicals, mg/L			Flocculation		Filtered Water[c]		
pH	Absorb-ance	Total[a] Mn ppb		Coag.	Flocc.	pH[b]	Floc Size	Residual Mn ppb	%	Absorb-ance
6.9	0.228	351.0		alum, 10.0	LT20, 0.1	6.4	C	24.9	7.1	0.013
6.9	0.228	351.0		alum, 20.0	LT20, 0.1	6.3	G	34.1	9.7	0.010
6.9	0.228	351.0		alum, 20.0	LT24, 0.1	6.3	G	36.1	10.3	0.009
6.9	0.228	351.0	Ca, 100.0	alum, 10.0	LT20, 0.1	6.4	D	33.0	9.4	0.012
6.9	0.210	369.0		alum, 10.0	C573, 0.1	6.5	D	36.8	10.0	0.012
6.9	0.210	369.0		C573, 20.0		6.6	<A	185.0	50.0	0.049
6.9	0.210	369.0		alum, 10.0	Ultrion, 0.1	6.5	B	37.6	10.2	0.014
6.9	0.210	369.0		Ultrion, 20.0		6.6	F	26.2	7.1	0.010
6.7	.214	367.0		Ultrion, 8.0		6.6	Nil			
6.7	.214	367.0		Ultrion, 12.0		6.6	Nil			
6.7	.214	367.0		Ultrion, 16.0		6.6	D	17.5	4.8	.012
6.7	.214	367.0		Ultrion, 28.0		6.6	F	17.7	4.8	.010
6.7	.214	367.0		Ultrion, 36.0		6.6	F	22.0	6.0	.010

[a] Raw water samples were spiked with $MnCl_2$ to give an additional (nominal) 200 ppb Mn. $KMnO_4$ was added at 137 ppb Mn (nominal).
[b] Sometimes samples were adjusted using an appropriate amount of sulphuric acid or sodium carbonate solution.
[c] Using 3 μm membrane filter.

3.3.2 Effect of pH

The results of a laboratory study on the effect of flocculation pH on the efficiency of removal of particulate manganese from raw water samples from Wyong are shown in Figure 3.4. Potassium permanganate was added to the water sample 10 minutes before the addition of alum. The results indicate that increasing the flocculation pH has the effect of improving the removal of particulate manganese. At the same time, it has the effect of decreasing the colour removal efficiency. Maximum colour removal is obtained at flocculation pH values <6.5, while maximum Mn removal is obtained at pH >6.5. Water in the flocculation tanks at the Wyong Shire Water Treatment Plant is usually maintained at about the optimal pH for combined colour and manganese removal with values in the range 6 to 6.5.

3.3.3 Effect of organics

Naturally ocurring organic compounds (humic and fulvic acids) have been reported to significantly increase the amount of primary coagulant required for optimal performance of the flocculation process (Narkis and Rebhun, 1983). Indeed, Bursill et al. (1985) reported that for South Australian waters with high organic contents (5-25 mg/L), the nature and concentration of these compounds are generally the most important factors determining the chemical requirements for flocculation. These investigators obtained a linear relationship between the dissolved organic carbon concentration and the alum dose required for optimum floc formation and attributed the increase in required alum dose to preferential reaction of the coagulant with the humic materials. Amy et al. (1989) indicate that the formation of both dissolved and precipitated aluminium-organic entities may indeed consume coagulant. In addition, it is possible that the formation of an organic coating on the particles to be removed with an associated increase in surface charge (and thence neutralisation requirement) could also result in increased consumption of coagulant. Dempsey (1989) also notes that organic compounds may coat the freshly formed aluminium hydroxide particles thus rendering them more stable.

In addition, and perhaps most importantly, natural organic matter may adsorb to the colloidal iron and manganese oxides generated in the oxidation process. Such adsorption will impart a negative charge to the particles, possibly resulting in increased stability (with the concomitant effect that destabilization may require larger

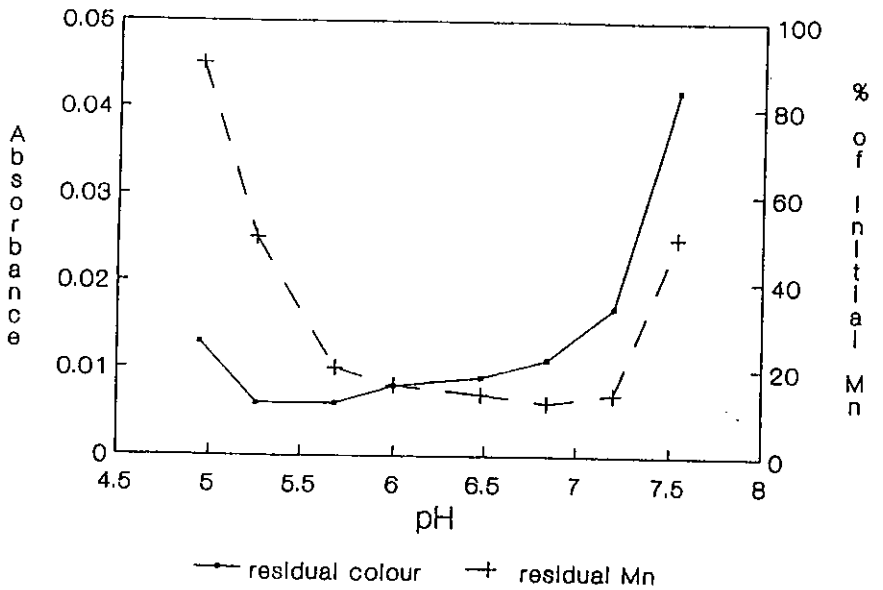

Figure 3.4. Effect of flocculation pH on removal of manganese and colour (as measured by absorbance at 416 nm). Laboratory-based investigation using raw water from Wyong Shire water treatment plant.

concentrations of coagulant). The increase in charge on particles nucleating within the water treatment plant (i.e. on addition of oxidant) may also result in the generation of smaller sized particles.

Investigations in which aliquots of Mardi Dam waters were spiked with varying concentrations of fulvic acid indicated that even at a low concentration of 1 mg/L (which is equivalent to a DOC of approximately 0.5 mg/L), alum dosing had to be doubled for flocculation to occur (Table 3.3).

Table 3.3
Effect of fulvic acid addition on floc size and manganese removal efficiency using raw water to the Wyong Shire water treatment plant.

			Filtered Water[b]			
Fulvic acid[a]	Alum	Floc size	Abs	Mn	Fe	Al
mg L^{-1}	mg L^{-1}	mm		ppb	ppb	ppb
0.0	10.0	4	0.007			
1.0	10.0	none				
2.0	10.0	none				
0.0	20.0	4	0.008	5.6	1.2	7.5
1.0	20.0	4	0.007	6.0	1.7	10.4
2.0	20.0	4	0.008	6.2	2.1	16.1
4.0	20.0	1	0.016	6.0	2.5	27.0

a Added to raw water of 28.7 ppb Mn, 0.07 Absorbance (Abs).
b Using 3 μm membrane filter

Although the concentrations of metals (Mn, Fe and Al) shown in Table 3.3 are not high, the observed increase in the metal concentrations in the filtered water as the concentration of added fulvic acid increases may indicate significant complexation of

these metals by fulvic acid. Alternatively, it could also indicate a fulvic acid-induced increase in charge on the oxide particles preventing them from aggregating to larger filterable particles.

The addition of strong oxidants such as potassium permanganate or ozone may degrade a significant portion of the organic matter present thus lowering the requirement somewhat for coagulant. While cost is the obvious limiting factor, more consideration should be given to the use of these agents in place of chlorine for the combined purpose of organics and manganese control, particularly in view of the inefficiency of the oxidation of Mn(II) by chlorine and the increasing awareness of problems associated with trihalomethanes in potable waters.

3.4 Filtration

The optimal water treatment process will be dependent to a large extent on the size and concentration of particles in the raw water and three types of treatment are typically considered; (1) Contact filtration, in which destabilizing chemicals are added to the raw water and the destabilized suspension is applied to the filters without further processing; (2) direct filtration, in which the destabilized suspension is flocculated to accomplish particle growth prior to filtration; and (3) conventional treatment, in which destabilization, flocculation and sedimentation precede filtration.

The boundaries between areas in which specific process configurations dominate with respect to minimizing costs are shown in Figure 3.5 as functions of the mass concentration of particles in the raw water (mg/L) and the size (volume average diameter, μm) of the particles in that water (after Wiesner, 1985). Note that, in this analysis, the destabilizing chemicals are considered to contribute minimal solid volume to the water being treated. Direct filtration has two distinct areas of application. In the lower region (small particles and low concentrations), flocculation provides sufficient particle growth to reduce the head loss caused by small particles. In the upper region, flocculation again permits higher filtration rates by reducing the head loss caused by the particles applied to the filter. Contact filtration is optimal at very low particle concentrations. This is because excessively long flocculation periods are needed to produce particle aggregation in such dilute suspensions. When conventional filtration is optimal, sedimentation is required to remove particles prior to filtration. Particles are removed at less cost by adding settling tanks than by building larger filters in this region.

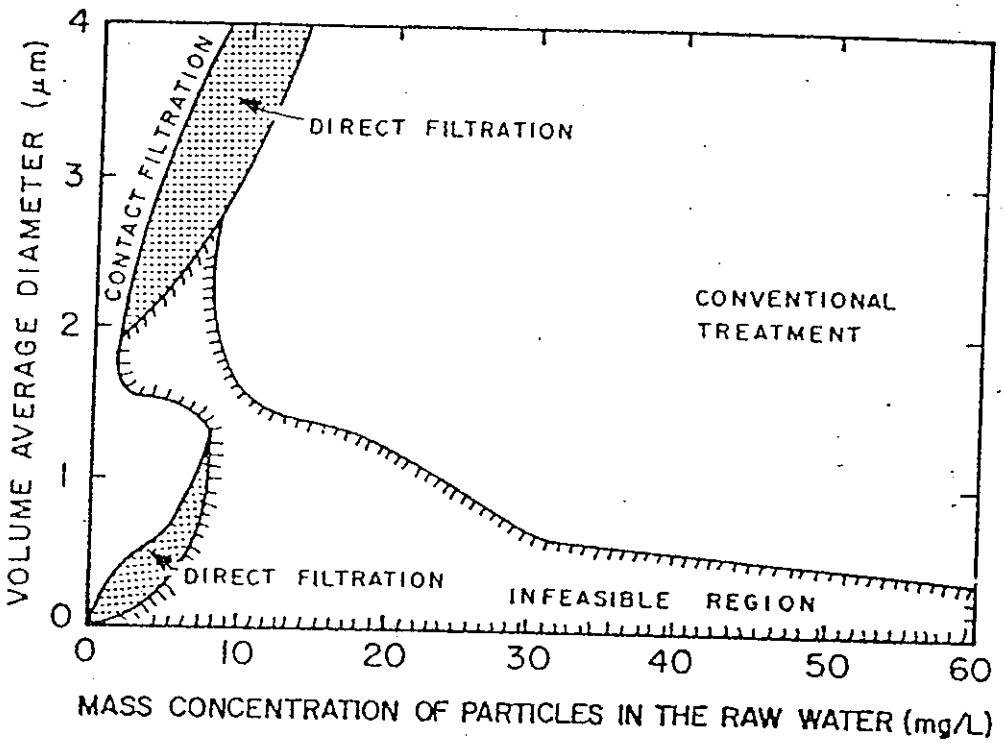

Figure 3.5. Optimal water treatment configuration as a function of raw water characteristics (particle size and concentration). Shaded areas correspond to direct filtration as optimal configuration (after Wiesner, 1985).

O'Melia (1985) notes that it is also useful to describe filtration as favourable or unfavourable, depending upon solution chemistry and the surface characteristics of the suspended particles and the filter media. In favourable filtration, there are no repulsive interactions as suspended particles reach the surface of the filter media. This could arise, for example, when the particles and the collectors have opposite charges, as in the filtration of positively charged ferric hydroxide by negatively charged sand at a pH of 6. In unfavourable filtration, a net repulsive interaction between particles and collector will effect attachment substantially. This could arise, for example, when the suspended particles and the collector have similar charges, as in the filtration of many clays by clean sand at a pH of 7.

Direct filtration plants, in conjunction with pre-oxidation processes, have been successfully used for the removal of iron and manganese in many locations (e.g. Waite *et al.*, 1989a; Bratby, 1988) though operating conditions suitable for the removal of colour and turbidity to acceptable levels may not always be optimal for removal of iron and (particularly) manganese. Consider, for example, the results of studies conducted at the Wyong water treatment plant. Excessively short filter run times were observed due to clogging of filter pores and surface mat formation. The Wyong treatment plant contains six filters which, for most of the plant lifetime, have incorporated deep beds of uniform dual media consisting of 375 mm of 0.55 mm diameter sand topped with 900 mm of 1.25 mm diameter anthracite. The design filtration rate for these filters is 3.9 L/s/m^2 but, due to the high water demand (particularly during the summer months), and the shorter than expected run times for filters when operating at their design filtration rate, frequently operate at significantly higher rates - a situation which accelerates head loss.

The short filter run times experienced at Wyong prompted engineers to recommend the increase in diameter of anthracite particles in one of the filter units to 1.75 mm. Such a change would be expected to increase filter run times but, because of the decrease in surface area and the increase in pore size, could result in lower trapping efficiency for particles such as manganese, iron and aluminium oxides. To test this possibility, sampling and subsequent analysis of the effluent of the filters was carried out following filter backwashing and was continued at frequent intervals for a period of up to 8 hours.

The results of these studies are shown in Figures 3.6 - 3.8. The initial poor quality of treated waters following backwashing is a common feature of many water treatment plants and is a function of both the composition of the water remaining in the filter at the end of backwashing and of the influent water quality (Francois and van Haute, 1985).

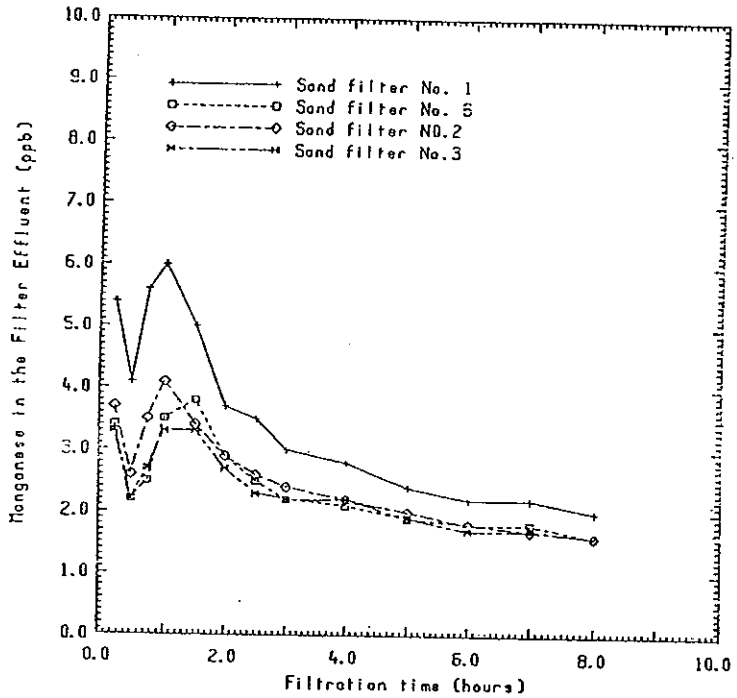

Figure 3.6. Manganese concentrations in the effluents of mixed media (anthracite and sand) filters of Wyong Shire water treatment plant as a function of filtration time following backwashing. Filter No.1 contained 1.75 mm diameter anthracite while all other filters contained 1.25 mm anthracite.

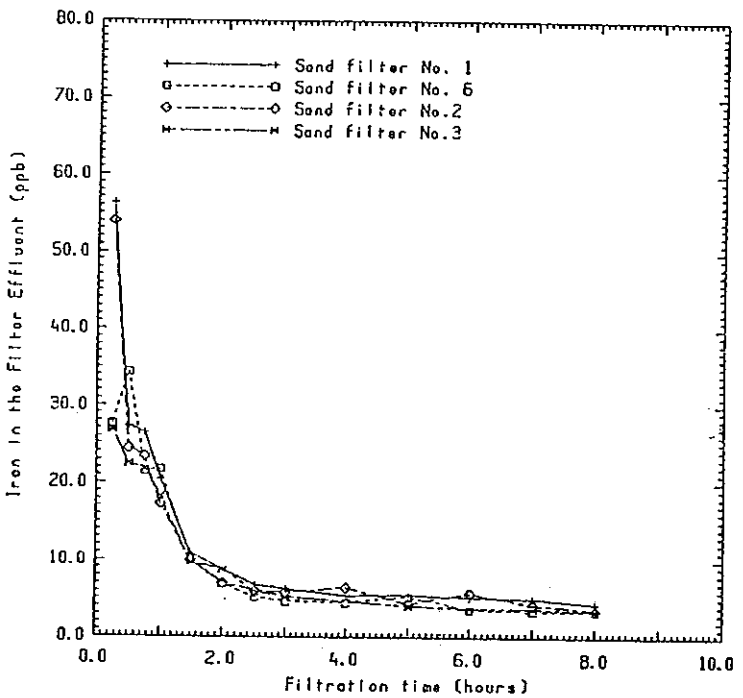

Figure 3.7. Iron concentrations in the effluents of mixed media (anthracite and sand) filters of Wyong Shire water treatment plant as a function of filtration time following backwashing. Filter No.1 contained 1.75 mm diameter anthracite while all other filters contained 1.25 mm anthracite.

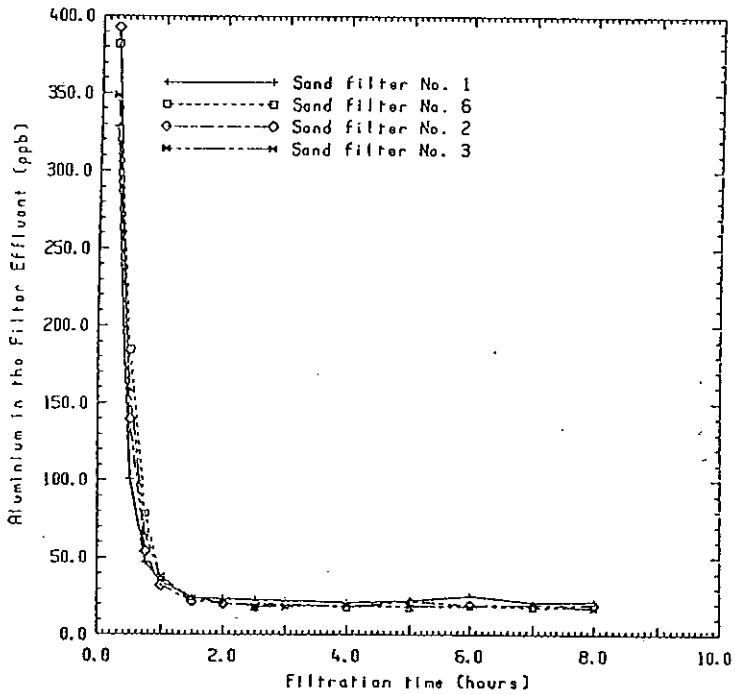

Figure 3.8. Aluminium concentrations in the effluents of mixed media (anthracite and sand) filters of Wyong Shire water treatment plant as a function of filtration time following backwashing. Filter No.1 contained 1.75 mm diameter anthracite while all other filters contained 1.25 mm anthracite.

The subsequent period of improvement (of about two hours duration), or filter ripening, has been related to the accumulation of influent particles within the pores of the media, resulting in increased capture of additional particles (O'Melia, 1985).

It is clear from Figure 3.6 that a change to the larger diameter anthracite does result in lower removal efficiencies for manganese (but not for iron or aluminium). In fact, once filter operation stabilised following backwashing, total manganese concentrations from Filter No. 1 (that possessing the larger diameter anthracite) were, on average, 27% higher than effluent concentrations from filters with the smaller anthracite particles (the percentage increase is significantly higher during the first two hours following backwashing). A similar study conducted on another occassion indicated a 55% increase in manganese concentration through the coarser media (though, in all cases studied, the effluent manganese concentrations were maintained below the target level of 20 ppb).

The importance of aging of the filter media and, in particular, the development of a manganese oxide coating has been stressed by Knocke *et al.* (1988) who carried out a laboratory-based study to evaluate the extent of soluble manganese removal by manganese oxide-coated anthracite and sand filter media. Filter column experiments using both new anthracite and sand as well as oxide-coated media obtained from full-scale water treatment plants were undertaken. Most pre-used media were found to have significant oxide coating, with typical extractable manganese contents of 2-5 mg Mn/g of media. In the absence of an applied oxidant, virgin sand or coal media had no significant Mn^{2+} removal capacity. In contrast, the efficiency of manganese removal by pre-used media was found to be governed by the filter influent pH (≥8.8) and the concentration of the surface MnO_x and its oxidation state.

Knocke *et al.* (1988) also reported that when prechlorination of the filter influent was carried out, effective manganese removal was observed when the pH was 6.1 or greater. They noted that >98% of the manganese in the prechlorinated filter influent water was still in the dissolved Mn^{2+} form. The sorptive removal capacity by the MnO_x coating on the filter media was thought to be mostly responsible for the manganese removal. Dissolved chlorine increases the oxidation state of the MnO_x coating which, in turn, improves its manganese adsorption capacity. The removal mechanism observed when stronger oxidants (permanganate, ozone) were used was different than when chlorine was utilised. In these cases, the oxidation of Mn^{2+} occurred almost immediately after the addition of oxidant. The filter media, thus, functioned as a collector for colloidal manganese oxides. This hypothesis was substantiated by the observed recovery of manganese during the

back-washing operation. When chlorine was used as an oxidant, very little of manganese was recovered. On the other hand, when stronger oxidants were used, the manganese recovery was much higher, indicative of the release of previously entrapped colloidal manganese oxide particles.

It should be noted that our ability to describe the capture efficiency of colloidal particles such as those of iron and manganese oxides on deep bed filters is not particularly strong. The attachment and subsequent removal of a suspended particle at the solid-liquid interface presented by a deep-bed filter is controlled by the surface properties of the particles to be removed and the filter medium (Chang and Vigneswaran, 1990). However, Elimelech and O'Melia (1989, 1990) have found that the classical Derjaguin-Landau-Verwey-Overbeek (DLVO) theory of colloid stability breaks down when attempting to describe the capture of colloidal particles on a filter medium and indicate that further work on the interfacial electrodynamics of interaction, coupling of electrodynamics and hydrodynamics and the possible effects of surface roughness and particle structure on particle capture is urgently needed.

3.5 Sequestration

Dart (1983) stated that, according to a 1970 survey assessment of filtration plants in the State of Nebraska, many plants failed to remove contaminants down to the 0.3 mg L^{-1} iron and 0.05 mg L^{-1} manganese recommended standards. One of the common causes of the failures was that the raw water iron already combined with naturally occurring silica and thus would not fully precipitate.

The fact that silica can prevent iron precipitation has therefore been used as a water treatment process. The procedure of injecting sodium silicate at the point of rapid oxidation of the ferrous to ferric iron has been described by Dart (1983) as a cost-effective sequestering method. It should be noted, however, that the presence of elevated stabilised iron and manganese in a water supply can still create problems if conditions in the distribution system permit breakdown of the sequestered material (e.g. long-term stagnation zones in a distribution system). Four sequestration procedures have been found practical for water treatment in Ontario. The use of sodium hexametaphosphate (or polyphosphate), sodium silicate or hydrogen peroxide (manganese only) have been suggested as sequestering agents. The choice of sequestration option is determined by:

- the concentration of iron or manganese (not to be greater than 2 to 3 mg L^{-1};

- the ease of oxidising of each contaminant: waters with easily oxidisable contaminants can be treated with silicate, while those with slow to oxidise are treated with polyphosphate;
- sequestration control of iron and manganese is not recommended for waters which tend to support biological growth; the addition of polyphosphate may aid biological fouling if phosphate is actually the limiting nutrient for growths.

Manganese is less controllable by sequestration treatment than iron (Robinson and Ronk, 1987). These authors studied the sequestering of manganese by the nearly simultaneous additions of sodium silicate and sodium hypochlorite. Under conditions of close-to-neutral pH and 150-250 mg L^{-1} of alkalinity (as $CaCO_3$), 1 to 2 mg L^{-1} of manganese could be sequestered for up to one day.

4 RETICULATION SYSTEM

A major consequence of excessive iron and manganese concentrations entering the distribution system is the accumulation of a coating containing high concentrations of manganese, iron, aluminium, calcium, silica and organic matter. The deposition of manganese may occur by physicochemical processes and/or as a manganese depositing biofilm by microbial processes. Physicochemical deposition occurs in water distribution areas with sufficient chlorination (such as those near the water treatment plant) when manganese concentrations continuosly exceed 0.02 mg L^{-1} for a few days. Manganese depositing biofilm develops in areas of the water reticulation system with insufficient residual chlorine to control microbial growth (Sly et al., 1989). The microorganisms may be actively involved in the deposition of manganese through oxidation of Mn(II). Such "biological manganese oxidation" in the water distribution system appears to be caused by the presence of a *Hyphomicrobium*-like bacterium *Pedomicrobium manganicum* and a *Metallogenium*-like bacterium in attached biofilms. Further details of the various types of distribution system biofilms and the conditions under which they arise is given in publications by Sly and coworkers (Sly, 1987; Sly et al., 1988a).

Scouring of manganese oxide coatings is typically initiated by sudden increases in flow rate (Phey and Philips, 1989). Once detachment occurs the passage of these coatings through the distribution system would very likely cause abrasive shearing of other biofilm. Penetration of chlorine into an area of the distribution system insufficiently chlorinated to control biofilm growth, or a change in the water disinfection practice (from chlorination to chloramination) will also cause detachment of manganese-depositing biofilm (Cooper, 1989). In well established biofilm, sloughing will probably be confined to the outer layer of actively growing microorganisms.

As indicated earlier, Sly and coworkers (Sly, 1987; Sly et al., 1988a) found that dirty water complaints were registered in the Gold Coast region once manganese levels in the distribution system exceeded 0.02 mg/L. In light of this, Sly recommended that manganese levels entering the distribution system do not continuously exceed 0.01 mg/L. Sly also recommended that chlorination (or chlorine dioxide) levels in a water distribution system with potential manganese problems should be maintained at a level sufficient to control the growth of manganese-depositing biofilm while minimizing the formation of manganese oxide coating. The WHO recommended range of 0.2-0.5 mg L^{-1} chlorine is adequate (Sly et al., 1988b).

5 CONCLUSIONS AND RECOMMENDATIONS

"Dirty water" problems associated with the presence of high concentrations of iron and, in particular, manganese in potable waters appear to be occurring increasingly frequently in Australia with consumer complaints arising when manganese and iron rich biofilms slough off water distribution pipelines. Indeed, it is apparent that a large number of distribution systems throughout Australia constitute significant reservoirs of manganese (and iron) rich deposits which, at some stage in the future (under the impact of increased flows, increased inputs of these oxide forming elements or simply through the slow, gradual buildup of deposits) will begin releasing these troublesome materials to consumers.

While the maintenance of moderate, uniform chlorine residuals throughout the distribution system is essential in controlling biofilm growth, effective long-term management requires that concentrations of manganese and iron entering the distribution system be minimized. Both management of raw water source and optimization of treatment plant procedures for the removal of manganese and iron will be necessary in most cases to achieve this objective. Optimal procedures of reservoir and reticulation system management and treatment plant operation for the removal of these elements is very much case specific and requires an understanding of the chemical, biological and engineering aspects of the problem.

A number of more specific conclusions and associated recommendations have been formulated through this project and are documented below:

- Manganese and iron problems in most instances have been attributed to the extraction of hypolimnetic waters from thermally stratified reservoirs. While the implementation of artificial destratification within water supply reservoirs as a means of overcoming this problem is strongly supported, it is considered that greater understanding of the timescale of oxidation and sedimentation within fully mixed reservoirs is needed. Only when this information is available will it be possible to realistically assess the iron and manganese loads that can be placed on the reservoir and, concomitantly, the limits that should be placed on iron and manganese concentrations in source waters;
- In most Australian treatment plants in which some method of iron and manganese control is implemented, the raw waters entering the plant are monitored at regular intervals (and in some cases continuously) for iron and manganese concentrations. However, the currently adopted standard colorimetric methods, particularly for manganese, may lead to significant overestimation of concentrations present and caution in data interpretation must be exercised. Improved colorimetric methods for manganese (such as the porphyrin

method) and relatively inexpensive atomic absorption instruments are now available and consideration should be given to their use by water authorities concerned with iron and manganese. Additionally, the water treatment method adopted will be dependent on the form of the element present and analytical techniques that provide information on chemical speciation must be adopted.

- Reduced, soluble forms of iron and manganese (Fe(II) and Mn(II)) may occur in source waters and require the use of oxidants to convert to the particulate, oxidised form. While oxygen or chlorine are satisfacory oxidants for Fe(II), more powerful oxidants are required for the oxidation of Mn(II). The use of potassium permanganate is recommended for the oxidation of Mn(II), though the increasingly widespread use of ozone in water treatment suggests that the dynamics of interaction of this reagent with manganese be further investigated.

- In addition to the requirement for oxidation of Mn(II) and Fe(II) to insoluble particulate species, the oxides so formed must aggregate to sizes large enough to either sediment efficiently or, in the absence of a sedimentation stage, be trapped on the filter media being used. Our ability to describe the dependency of aggregate size on solution conditions for relatively simple systems is adequate but considerably more work is required in understanding the interactions in more complex systems typical of the water treatment plant.

- The addition of strong oxidants such as potassium permanganate or ozone may degrade a significant portion of the organic matter present thus lowering the requirement somewhat for coagulant. While cost is the obvious limiting factor, more consideration should be given to the use of these agents in place of chlorine for the combined purpose of organics and manganese control, particularly in view of the inefficiency of the oxidation of Mn(II) by chlorine and the increasing awareness of problems associated with trihalomethanes in potable waters.

- Direct filtration plants, in conjunction with pre-oxidation processes, have been successfully used for the removal of iron and manganese in many locations though operating conditions suitable for the removal of colour and turbidity to acceptable levels may not always be optimal for removal of iron and (particularly) manganese.

- Our ability to describe the capture efficiency of colloidal particles such as those of iron and manganese oxides on deep bed filters is not particularly strong. Further work on the interfacial electrodynamics of particle0filter interaction, coupling of electrodynamics and hydrodynamics and the possible effects of surface roughness and particle structure on particle capture is urgently needed.

- Following the recommendation of Sly and coworkers (Sly, 1987; Sly et al., 1989b) it is suggested that manganese levels entering the distribution system sould not continuously exceed 0.01 mg/L. We also strongly endorse the recommendation that chlorination levels in a water distribution system with potential manganese problems should be maintained at a level sufficient to control the growth of manganese-depositing biofilm while minimizing the formation of manganese oxide coating.

6 REFERENCES

Abukhudair M.Y., Farooq S. and Hussain M.S. (1989) Kinetics of ozonation of iron(II) and manganese(II). *J. Environ. Sci. Health,* A24(4), 389-407.

Aldridge, P., Chiswell, B., Leigh, M.K., O'Halloran, K.R. and Pascoe, *M.* (1989). *Water, Journal of the Australian Water and Wastewater Association* **15,** 35-37.

Amy, G.L., Collins, M.R., Kuo, C.J., Chowdhury, Z.K. and Bales, R.C. (1989). Effects of humic substances on particle formation, growth and removal during coagulation. In *Aquatic Humic Substances: Influence on Fate and Treatment of Pollutants*, I.H. Suffet and P. Macarthy (Eds), ACS Advances in Chemistry Series 219, American Chemical Society, Washington, DC, Chapter 27, pp 443-452.

APHA *(1980). Standard Methods for the Examination of Water and Wastewater.* American Public Health Association, American Water Works Association and the Water Pollution Control Federation, 15th Edition, Washington.

Asaeda, T and Imberger, J. (1988). Structures of bubble plumes in stratified environments. Environmental Dynamics Rept. ED-88-250, Centre for Water Research, University of Western Australia.

AWWA (1987). Research needs for the treatment of iron and manganese. Report of the AWWA Trace Inorganic Substances Committee. *J. AWWA* **79,** 119-122.

Baker, F.C. (1986). *L.G.E.A. Annual Conference Proceedings* **2,** 1-2.

Bowles, B.A., Powling, I.J. and Burns, F.L. (1979). Effects on water quality of artificial aeration and destratification of tarago Reservoir. Australian Water Resources Council Technical Report No. 46.

Bratby J.R. (1988) Optimizing manganese removal and washwater recovery at a direct filtration plant in Brazil. *J. AWWA* **80,** 71-81.

Brown, I. K. (1986). Review of the application of aeration/destratification techniques in Australia surface water storages. Dept. of Local Govt. Queensland, 55pp.

Brown, I. K. and Jory, A. G. (1983). The use of artificial mixing to control iron and manganese in Urban supply storages. Proc. 3rd Nat. Local Govt. Engineer Conf. Mebourne. The Inst. of Engineers Aust. Preprints of Papers, 146-151 (The Inst. of Engineers Aust., National Conf. Pub. No. 85/14).

Burns, F.L (1977). Localised destratification of large reservoirs to control discharge temperatures. *Progress in Water Technology* **9**, 53-63.

Bursill D.B., Hine P.T. and Moran J.Y. (1985) The effect of natural organics on water treatment processes. AWWA 11th Fed. Conv., Melbourne.

Carlson M.A., Hoehn R.C., Knocke W.R., Hair D.H. (1986). Experiences with the use of chlorine dioxide and potassium permanganate as preoxidants for trihalomethane and manganese control. Ann. Conf. Proc. AWWA, June 22-26, 1986, Denver Co., p 319-345.

Chang, J.S. and Vigneswaran, S. (1990). Ionic strength in deep bed filtration. *Water Res.* **24**, 1425-1430.

Chédal J. (1984) Raw water Preozonation. In *Handbook of Ozone Technology and Applications. Volume II. Ozone for Drinking Water Treatment.* (Rice R.G. and Netzer A. eds.) Butterworth Publisher.

Chiswell, B. and Zaw, M. (1989). The nature of iron and manganese species in dam waters. *Hydrological Processes* 3, 277-288.

Chiswell, B and Zaw, M. (1990). Lake Destratification and Speciation of Iron and Manganese, Forth Symposium on Our Environment, Singapore, May.

Colthurst J.M. and Singer P.C. (1982) Removing trihalomethane precursors by permanganate oxidation and manganese dioxide adsorption. *J. AWWA* Research ant Technology Febr. 1982 pp 78-83.

Cooper, P. (1989). Engineering and Water Supply Authority of South Australia. Private communication.

Cromley J.T. and O'Connor J.T. (1985) Effect of ozonation on the removal of iron from a ground water. In Ozone in Water Treatment- Applications, Operations, and Technology. AWWA Technical Resource Book. AWWA Denver Co.

Dart F.J. (1983) Recent developments in iron and manganese control. *Proceedings AWWA Seminar on Control of Inorganic Contaminants.* Las Vegas 1983 p.51-62.

Dempsey, B.A. (1989). Reactions between fulvic acid and aluminium: effects on the coagulation process. In *Aquatic Humic Substances: Influence on Fate and Treatment of Pollutants*, I.H. Suffet and P. Macarthy (Eds), ACS Advances in Chemistry Series 219, American Chemical Society, Washington, DC, Chapter 25, pp 409-424.

Dentel, S.K. and Gossett, J.M. (1988). Mechanisms of coagulation with aluminium salts. *J. AWWA* **80**, 187-198.

Earp, G.N.S., Jackson, J.R. and Evans, I.R. (1985). Investigation and design of engineering works for development of the groundwater resources of Barwon Downs. Proceedings of the Australian Water and Wastewater Association 11th Federal Conference, Melbourne.

Elimelech, M. and O'Melia, C.R. (1990a). Effect of particle size on collision efficiency in the deposition of Brownian particles with electrostatic energy barriers. *Langmuir* **6**, 1153-1163.

Elimelech, M. and O'Melia, C.R. (1990b). Kinetics of deposition of colloidal particles in porous media. *Environ. Sci. Technol.* **24**, 1528-1536.

Emerson, S. Kalhorn, L. Jacobs, B.M. Tebo, K.H. Nealson and R.A. Rosson (1982). *Geochim. Cosmochim. Acta* **46**, 1073-1079.

Ficek, K.J. (1978). Potassium permanganate for iron and manganese removal and taste and odor control. In *Water Treatment Plant design for the Practicing Engineer*, R.L. Sanks (Ed.), Ann Arbor Science, Ann arbor, Michigan.

Francois, R.J. and van Haute, A.A. (1985). Backwashing and conditioning of deep bed filters. *Water Res.* **19**, 1357.

Georgeson D.L. and Karimi A.A. (1988) Water quality improvements with the use of ozone at the Los Angeles water treatment plant. *Ozone Science & Engineering* **10**, 255-276.

Ho, W. K. C. and Murray, B. A. (1984). Artificial destratification of rocky Creek Dam. Water supplied and resources conference, Sydney, Loacal Government Association. 109-121.

Ireland, R.W. (1986). South Coast water Quality Investigation; Scientific Services Sub-Branch, Sydney Water Board, June.

Ishii, H., Koh, H. and Satoh, *K. (1982). Anal. Chim. Acta,* **136**, 347-352.

Jenkins S.R., Benefield L., Keal M.J. and Peacock R.S. (1984) Effective manganese removal using lime as additive. *J. AWWA* **76**, 82-86.

Kawashima, M., Takamatsu T. and Koyama M *(1988). Water Res.* **22**, 613-618.

Khoe G.H. and Waite T.D. (1989) Manganese removal from Wyong water supply. 13th Fed. Conv. of the AWWA, Canberra. National Conf. Publ. No. 89/2, The Inst. of Engrs. Australia.

Knocke W.R., Hoehn R.C. and Sinsabaugh R.L. (1987) Using alternative oxidants to remove dissolved manganese from waters laden with organics. *J. AWWA* **79,** 75-79.

Knocke W.R., J.R. Haman and C.P. Thompson, *J. AWWA 80,* 65-70 (1988).

Kruithof J.C., van der Gaag M. and van der Kooy D. (1989) Effect of ozonation and chlorination on humic substances in water. In *Aquatic Humic Substances* (Suffet I.H. and MacCarthy P. eds.), pp 663-680. Advances in Chemistry Series 219. American Chemical Society, Washington DC.

Letterman, R.D. and Vanderbrook, S.G. (1983). Effect of solution chemistry on coagulation with hydrolysed Al(III). *Water Res.* **17,** 195.

Loos, E. T. (1987) Experiences with manganese in Queensland water supplies. Water, Journal of the Australian Water and Wastewater Association **14,** 28-37.

Lowther, I.M. and Evans, I.R. (1980). Report on pilot treatment plant for iron removal from groundwater. Unpublished internal report of the Geelong and District Water Board.

McAuliffe, T. F. and Rosich, R. S. (1990). The triumphs and tribulations of artificial mixing in Australian water bodies. *Water* **31,** 22-23.

McAuliffe, T.F. and Rosich, R.S. (1989). A review of the effects of artificial destratification on water quality in Australian water storages. Urban Water Research Association Research report No. 9, 233 pp.

Narkis N. and Rebhun M. (1983) Inhibition of flocculation processes in systems containing organic matter. *J. Wat. Pollut. Control Fed.* **55,** 947-955.

O'Melia, C.R. (1985). Particles, pretreatment and performance in water filtration. *ASCE J. Environ. Eng.* **10,** 167.

Paillard H., Legube B., Bourbigot M.M. and Lefebre E. (1989) Iron and manganese removal with ozonation in the presence of humic substances. *Ozone Science & Engineering* **11,** 93-114.

Paillard H., Legube B. and Doré M. (1989a) Effects of alkalinity on the reactivity of ozone towards humic substances and manganese. *Aqua* **38,** 32-42.

Pascoe M. and Loos T. (1990) Chlorine dioxide- The American experience. *Water* **17,** 48.

Phey B. and Philips, C. (1989). *Manganese slime deposition and removal from 2100 mm diameter Winneke/Preston main.* Paper presented at 13th Federal Convention of the Australian Water and Wastewater Association, Canberra March 6-10 (1989). National Conference Publication No.89/2, The Institution of Engineers, Australia.

Posselt H.S., Reidies A.H. and Weber W.J. (1968) Coagulation of hydrous manganese dioxide, *J. AWWA* **60**, 48-68.

Raman, K. R. and Arbuckle, B. R. (1989). Long-term destratification in an Illinois lake, *J. AWWA* 80, 66-71.

Robinson, R.B., Minear R.A. and J.M. Holden (1987) *J. AWWA* **79**, 116-125.

Robinson R.B. and Ronk, *S.K. (1988). J. AWWA* **80**, 64-70.

Robinson R.B. and Ronk S.K. (1987) The treatability of manganese by sodium silicate and chlorine. *J. AWWA* **79**, 64-70.

Sly, L.I, (1987). *Investigation into biological manganese oxidation and deposition in the Gold Coast water distribution system.* UniQuest Limited, University of Queensland.

Sly, L.I., Arunpairojana V. and Hodgkinson, M.C. (1988a). *Systematic and Applied Microbiology, 11,* 75-84.

Sly, L.I., Hodgkinson M.C. and Arunpairojana, V. (1988b). *FEMS Microbiology Ecology, 53,* 175-186.

Sly, L.I., Chiswell, B., Hamilton, G.R., Dixon, D.R., Waite, T.D. and Willoughby, G. (1989a). Report to Pine Rivers Council on Investigation into Manganese Related and Other Water Quality Problems, pp 1-188.

Sly, L.I., Hodgkinson M.C. and Arunpairojana, V. (1989b). *The control of manganese deposition and "dirty water" in the Gold Coast water distribution system.* Paper presented at 13th Federal Convention of the Australian Water and Wastewater Association, Canberra March 6-10 (1989). National Conference Publication No.89/2, The Institution of Engineers, Australia.

Staehelin, J. and Hoigne, J. (1985). Decomposition of ozone in water in the presence of organic solutes acting as promoters and inhibitors of radical chain reactions. *Environ. Sci. Technol.* **19**, 1206-1213.

Stoebner R.A. and Rollag D.A. (1985) Ozonation of a municipal groundwater supply to reduce iron, manganese, and trihalomethane formation. In Ozone in Water Treatment-Applications, Operations, and Technology. AWWA Technical Resource Book. AWWA Denver Co.

Stubbings, J.A., Waite, T.D. and Raper, J.A. (1987). Investigation of colloid aggregation kinetics by photon correlation techniques. Proceedings of 6th Australian Conference on Colloids and Surfaces, Sydney, August.

Stumm, W. and Morgan, J.J. (1981). Aquatic Chemistry. Wiley, New York.

Thomas, P. (1985). Manganese removal from potable water. Unpublished internal report of the State Water Laboratory, Engineering and Water Supply Department, South Australia, Report No. 159/84.

US EPA (1989) *Health effects of drinking water treatment technologies*. Drinking water health effects task force. Office of Drinking Water, U.S. Environmental Protection Agency, Washington D.C.

Viraraghavan, T., Winchester, E.L., Brown, G.J., Wasson G.P. and Landine, *R.C. (1987). J. AWWA* 79, 43-48.

Waite, T.D., Sly, L.I., Khoe, G., Dixon, D.R., Chiswell, B. and Batley, G.E. (1989a). Manganese-related water quality problems in the Wyong Shire region of New South Wales. Australian Nuclear Science and Technology Organisation Report No. ANSTO/C98.

Waite, T.D., Sly, L.I., Khoe, G.H., Dixon, D.R., Chiswell B. and Batley, G.E. (1989b). *Manganese and iron related problems in water supplies- Observations and research needs.* Proceedings of the 13th Federal Convention of the Australian Water and Wastewater Association, Canberra March 6-10 (1989). National Conference Publication No.89/2, The Institution of Engineers, Australia.

Waite, T.D. and Morel, F.M.M. (1984). Ligand exchange and fluorescence quenching studies of the fulvic acid-iron interaction. Anal. Chim. Acta **162**, 263-274.

Weast R.C. (1977) Handbook of chemistry and physics. CRC press.

Weissenhorn F.J. (1984) Removal of iron and manganese by ozone during drinking water treatment in Dusseldorf. In *Handbook of Ozone Technology and Applications. Volume II. Ozone for Drinking Water Treatment*, Rice R.G. and Netzer A., Eds, Butterworth Publishers.

Weng, C., Hoven, D.L. and Schwartz, B.J. (1986). Ozonation: an economic choice for water treatment. J. AWWA **78**, 83-90.

Wiesner, M. (1985). Optimal water treatment plant configuration: effects of raw water characteristics. PhD Thesis, Johns Hopkins University.

Wong J.M. (1984) Chlorination-filtration for iron and manganese removal. *J. AWWA* **76**, 76-79.

Yapijakis, C. (1986). Removal of iron and manganese from drinking water using an innovative method. Proc. Int'l Conf. on Chemicals in the Environment, Lisbon, Portugal, July, pp. 822-829.

7 APPENDICES

7.1 Appendix 1: Kinetics of Aggregation of Colloidal Iron Oxides

INTRODUCTION

The aggregation kinetics of fine particles has been an area of prime interest in colloid science for many years, with important implications for problems relating to air and water pollution control, as well as for a wide variety of natural and commercial processes. The study of colloidal aggregation phenomena has been made easier with the advent of new instruments based on techniques utilizing the availability of large capacity, high speed computers. One of these techniques, Photon Correlation Spectroscopy (PCS), has been used in the present work to measure the change in particle size distribution with time and hence to study the aggregation kinetics of haematite particles. Previous work which used PCS for the measurement of particle size in aggregating systems concentrated on the initial stages of aggregation in which single particles combine to form doublets (1). In this work, however, long times are considered so that multiplets are also formed. The aggregation results obtained from the light scattering experiments are compared with the predictions of a theoretically derived model in which Smoluchowski's kinetic equation (2) has been modified using a rate constant determined from the repulsion and attraction energies and account is taken of the nature of packing within the aggregate structure.

PCS THEORY

Photon Correlation Spectroscopy has been used to measure the diffusion coefficient of colloidal particles in suspensions. The hydrodynamic radius can be determined from the diffusion coefficient as has been discussed in several excellent reviews (3,4). PCS determines particle size from the fluctuations in scattered intensity that occur over very short time intervals. The time dependence of this fluctuating intensity is governed by the random thermal or Brownian motion of the particles, expressed as the diffusion coefficient. The data required for particle size analysis by PCS are values of the intensity (photocount), $I(t)$, at some arbitrary time, t, and at some later time, $I(t+\tau)$, where τ is the difference in time between the two counts. From these two photocounts, the autocorrelation function, $C(\tau)$, is computed as the product of the two intensities, $C(\tau) = < I(t).I(t+\tau) >$, and the normalised autocorrelation function is given by $g^2(\tau) = \frac{< I(t)I(t+\tau) >}{< I(t)I(t) >}$. The first order autocorrelation function, $g^1(\tau)$, is related to the normalised autocorrelation function by $|g^1(\tau)|^2 = g^2(\tau) - 1$.

For monosized particles, $g^1(\tau)$ can be written as a single exponential function decaying to an infinite time value,

$$|g^1(\tau)| = \exp(-\Gamma\tau) \qquad [1]$$

where $\Gamma = DQ^2$. The translational z-averaged diffusion coefficient of the particle, D, is related to the hydrodynamic radius, R_h, by the Stokes-Einstein equation,

$$D = \frac{k_B T}{6\pi\eta R_h} \qquad [2]$$

where k_B is Boltzmann's constant, T is the absolute temperature, η is the viscosity of the surrounding medium. Q is the magnitude of the scattering vector, defined as

$$Q = \frac{4\pi n}{\lambda} \sin\left(\frac{\theta}{2}\right) \qquad [3]$$

where n is the refractive index of the medium, θ is the scattering angle, and λ is the incident wavelength of the light measured in vacuum. In practice, samples are typically polydisperse and this necessitates the use of a correlation function which is a distribution of exponential time constants,

$$|g^1(\tau)| = \int_0^\alpha G(\Gamma)\exp(-\Gamma\tau)d\Gamma \qquad [4],$$

where $G(\Gamma)$ is the normalized distribution in Γ space. There are three main approaches to analysis of PCS data: method of cumulants, fit to a known distribution function, and inversion of the Laplace transform (5). The approach used in this study is the method of cumulants (6), in which the right hand side of Eq. [4] is expanded in a series about the mean, $\bar{\Gamma}$:

$$|g^1(\tau)| = \exp(-\bar{\Gamma}\tau)\left(1 + \frac{\mu_2\Gamma^2}{2!} - \frac{\mu_3\Gamma^3}{3!} + \ldots\right) \qquad [5]$$

and can be analysed to give the values of $\bar{\Gamma}, \mu_2$.

Brown and Pusey (7) showed that a well defined averaged diffusion coefficient (z-average diffusion coefficient),

$$\overline{D_Z} = \frac{\bar{\Gamma}}{Q^2} = \frac{\sum N_i M_i^2 D_i}{\sum N_i M_i^2} \qquad [6]$$

where N_i is the number of particles i, M_i is the mass of a particle i, and D_i is the diffusion coefficient of i, was appropriate for small particles of diameter less than $\left(\frac{\lambda}{10}\right)$ and which exhibit negligible angular dependence on scattering. The diffusion coefficient may also be related to hydrodynamic size of the particle by using the Stokes-Einstein equation (Eq. [2]).

THE THEORETICAL MODEL

If a number of moving particles are confined within a certain volume of liquid, they may or may not collide with each other, depending on their number concentration and/or mutual affinity (repulsion/attraction). Assuming that they do collide, they may or may not adhere permanently to each other depending, again, on their mutual affinity and/or on the agitation characteristics of the medium. Here, only the case of irreversible adhesion of colliding particles will be considered. In this case, the agglomerate growth process can be described by a series of 'reactions' of the type:

$$n_i + n_j \rightarrow n_{i+j} \qquad [7]$$

where n_i, n_j and n_{i+j} are the number concentration of the 'reactants' and 'product' respectively. Following the analogy to chemical reactions, a rate constant, k_{ij}, for the aggregation can be defined as:

$$-\frac{dn_i}{dt} = -\frac{dn_j}{dt} = k_{ij} n_i n_j \qquad [8]$$

for $i \neq j$

$$\frac{dn_l}{dt} = k_{ij} n_i n_j \qquad [8a]$$

for $i = j$

$$\frac{dn_l}{dt} = \frac{1}{2} k_{ij} n_i n_j \qquad [8b]$$

where l = i+j, t is time and Eq.[8a,b] give the rate of formation of aggregates l. However, there is also a rate of 'consumption' of aggregates l as 'reactions' to form aggregates of higher order are occuring simultaneously. The balance of these 'reactions' is the classical Smoluchowski kinetic equation (8):

$$\frac{dn_l}{dt} = \frac{1}{2} \sum_{i=1, j=l-i}^{l-1} k_{ij} n_i n_j - n_l \sum_{i=1}^{\infty} k_{il} n_i \qquad [9].$$

Equation [9] can be numerically integrated to give the variation of the number of aggregates l with time, provided that a suitable expression for k_{ij} (and k_{il}) is used.

Brownian aggregation (rapid aggregation)

If the particles are indifferent to each other and sufficiently small to have negligible settling velocity, the only mechanism promoting collision between them is Brownian motion. In this case, the rate constant can be based on Fick's first law with the coefficient of diffusivity estimated from the Stokes - Einstein equation. The result can be written as (see 8):

$$k_{ij(r)} = \frac{2k_B T}{3\eta} \left(\frac{1}{r_i} + \frac{1}{r_j} \right) (r_i + r_j) \qquad [10]$$

where r_i, r_j are the radii of the aggregates. For a monodisperse system ($r_i = r_j$), the rapid rate constant is reduced to

$$k_{(r)} = \frac{8k_B T}{3\eta} \qquad [11]$$

and the Smoluchowski kinetic equation (eqn. 9) becomes,

$$\frac{dn_l}{dt} = \frac{1}{2} k_{(r)} \sum_{i=1, j=l-i}^{l-1} n_i n_j - k_{(r)} n_l \sum_{i=1}^{\infty} n_i \qquad [12].$$

The above equation can be solved analytically (8), and in general the concentration of the l^{th} aggregates can be represented by,

$$n_l = \frac{n_0 \left(\frac{1}{2} k_{(r)} t n_0 \right)^{l-1}}{\left(1 + \frac{1}{2} k_{(r)} t n_0 \right)^{l+1}} \qquad [13]$$

where n_0 is the initial particle concentration.

In many practical cases, however, the rate of aggregation is retarded by the presence of repulsive forces between the particles and the rate given by equation [10] grossly over-estimates the aggregates growth.

Slow aggregation

To account for the retardation in the rate of aggregation, a correction factor, known as the stability ratio, is defined as (1):

$$W_{ij} = \frac{k_{ij(r)}}{k_{ij}} \qquad [14]$$

where $k_{ij(r)}$ is given by equation [10] and k_{ij} is the corrected rate constant, to be used in equation [9]. The stability ratio can be determined by an expression derived by Füchs (9), that can be written as:

$$W_{ij} = (r_i + r_j)\int_{r_i+r_j}^{\infty} \frac{\exp\left(\frac{V_T(r)}{k_B T}\right)}{r^2} dr \qquad [15]$$

where r is the distance between the center of aggregates and $V_T(r)$ the total interactive energy between the pair of aggregates. The total interactive energy is given by:

$$V_T(r) = V_R(r) + V_A(r) \qquad [16]$$

where $V_R(r)$ is the repulsive and $V_A(r)$ the attractive energy of interaction, respectively.

The repulsive energy of interaction

The following expression, derived by Hogg, Healy and Fuerstenau (10) was used here:

$$V_R(H) = \frac{\pi\varepsilon_0\varepsilon_R r_1 r_2}{r_1 + r_2}\{(\psi_1 + \psi_2)^2 \ln\{1 + \exp(\kappa H)\} + (\psi_1 - \psi_2)^2 \ln\{1 - \exp(-\kappa H)\}\} \qquad [17]$$

where $V_R(r)$ is given in Joules, H is the distance between the surface of the particles in meters ($H=r-r_1-r_2$), ε_0 is the permittivity of vacuum, ε_r is the relative dielectric constant of the medium ($\varepsilon_r = 78.54$ for water at $25°C$), ψ_i is the surface potential of particle i (taken here to be identical to the zeta potential) and κ is the Debye-Hückel parameter given by:

$$\kappa = \left(\frac{2Ce^2z^2}{\varepsilon_0\varepsilon_r k_B T}\right)^{\frac{1}{2}} \qquad [18]$$

where z is the valence of the ionic species in solution, C the ionic concentration and e the electronic charge.

The attractive energy of interaction

For particles carrying like charges, the attraction between aggregates can be assumed to be due to Van der Waals forces. In terms of energy, the expression for the interaction between two aggregates of radius r_1 and r_2 is (11):

$$V_A(H) = -\frac{A}{12}\left\{\frac{y}{x^2+xy+x} + \frac{y}{x^2+xy+x+y} + 2\ln\left\{\frac{x^2+xy+x}{x^2+xy+x+y}\right\}\right\} \qquad [19]$$

where A is the Hamaker constant and $x = \frac{H}{2r_1}, y = \frac{r_2}{r_1}$.

Determination of the Hamaker constant is not a simple task. Its value depends on the composition of the aggregates and on the composition of the medium in which the particles are suspended. An approximate expression for estimating the effective Hamaker constant between two particles of a material, 2, embedded in a medium, 1, is (11):

$$A_{212} = \left(A_{11}^{\frac{1}{2}} - A_{22}^{\frac{1}{2}}\right)^2 \qquad [20]$$

where A_{11} and A_{22} represent the Hamaker constant of the particle and medium, respectively. Difficulty in using eqn.[20] arises because values of A are scarcely found in the literature and, in the case of water, reported values vary from $3.3\times10^{-20} - 6.4\times10^{-20} J$ (see 12).

In this work, the Hamaker constant was estimated experimentally utilizing a technique suggested by Barringer et al (13), which assumes irreversible transformation of singlets to doublets in the initial stages of aggregation (see Appendix).

Correlations for aggregate size

For the complete prediction of aggregate growth with time, it is necessary to attribute a size to the assembly of particles that constitutes each aggregate. If it is assumed that the aggregated particles meld together to form a single spherical particle containing the complete mass at the same density as the original colloid. The spherical equivalent volume for an aggregate of n primary particles (V_n) is given by:

$$V_n = nV_1 \qquad [21]$$

where V_1 is the volume of a primary particle in the dispersion. This means that the spherical equivalent radius is determined by:

$$r_n = n^{\frac{1}{3}} r_1 \qquad [22]$$

where r_1 is the radius of a primary particle. However, this concept is not supported by electron micrographs of aggregates which show that the structure of aggregates consists of quite distinct primary particles and retain their own individual shapes whilst in contact. Two different approaches were considered here:

(i) It was assumed that the growing aggregate did not change its packing structure with size. In this case, the spherical equivalent radius, r_n, of an aggregate composed of n singlets can be represented by:

$$r_n = \left(\frac{n}{f}\right)^{\frac{1}{3}} r_1 \qquad [23]$$

where f , the packing factor, is the ratio between the volume of the n singlets and the total volume of the aggregate which was taken as constant with aggregation time.

(ii) A fractal geometry for the growing aggregate was assumed. In this case, by definition, an aggregate of mass M contained within a radius R about its center can be described by (14):

$$M \propto R^{d_F} \qquad [24]$$

where d_F is the fractal dimension of the aggregate of value less than 3. If the primary particles remain intact upon aggregation, then the mass of an aggregate is proportional to the number of the primary particles, n, within it. Hence, the spherical radius of an aggregate composed of n particles is,

$$r_n = n^{\frac{1}{d_F}} r_1 \qquad [25].$$

It is worth noting that this assumption results in a decreasing packing density as the aggregate grows.

The theoretical average size of the aggregates is then estimated using the mass mean size equation,

$$\bar{r} = \frac{\sum f_i r_i^4}{\sum f_i r_i^3} \qquad [26].$$

where f_i is the number distribution of aggregates with i particles.

EXPERIMENTAL

Preparation of haematite

Samples of uniformly sized, approximately spherical haematite particles were prepared by forced hydrolysis of an homogeneous iron salt solution under strictly controlled conditions, as described by Matijevic and Scheiner (15) and slightly modified by Penners and Koopal (16). Details of the procedure are given elsewhere (17). Haematite samples were prepared and diluted to two different concentrations, 3.9×10^{-4} M and 1.95×10^{-4} M. These concentrations correspond to 4.5×10^{13} particles/litre and 2.25×10^{13} particles/litre assuming the presence of singlets only.

The regularity and sphericity of the particles is evident from a typical electromicrograph of the prepared haematite (see Figure 1).

Particle Size Analysis

The particle size distributions of the aggregating particles were measured with the Malvern 4700 PCS system, utilizing a 15 mW, 633 nm He-Ne laser. Two independent correlations were used to relate the intensity of the light scattered by each size population to its mass: the Rayleigh-Gans theory (18,19) and the more rigorous Mie theory (20) in which the refractive index of the particles and absorption function are taken into account. Both procedures were found to give comparable results. Figure 2 shows the particle size distribution of the haematite samples with a z-averaged diameter of approximately 100nm and a polydispersity index of 0.18.

Zeta potential measurements

The zeta potential of the particles was measured with the Malvern Zetasizer IIc system, which uses a 5 mW, 633nm He-Ne laser as light source. With this equipment, the particle scattered light is correlated to its electropheretic mobility, as an alternating electric potential with a known frequency is applied across the measurement cell. The particle zeta potential was then deduced from the measured electropheretic mobility using existing theory (21).

Aggregation experiments

Two sets of aggregation experiments were conducted, each using one of the prepared particle concentrations:4.5×10^{13} and 2.25×10^{13} particles/litre. In each set of experiments, several tests were performed with addition of a salt (KCl) to the agglomerating suspension. The salt concentrations ranged from 5 to 300mM. For each given salt concentration, the experimental test consisted of the measurement of particle size distribution versus time. The agglomeration was carried out in the sample reservoir of the particle sizer, so that size distributions were determined every 2-3 minutes without disturbing the process, the total experiment lasting up to 1 hour.

RESULTS and DISCUSSION

The result from the Malvern 4700 gives a z-average diameter, a polydispersity index, and intensity, mass and number weighted size distributions (see Fig. 2). The number distribution can be related to the hydrodynamic size using equation [26], and hence, the model aggregate size can be reasonably estimated from number distribution using equation [26].

Figures 3 and 4 show the variation of the measured aggregate size with time for the initial particle concentrations of 4.5×10^{13} and 2.25×10^{13} particles/litre, respectively. It can be seen that, in both cases, aggregate growth is extremely sensitive to salt concentration in the range between 20 and 50 mM. This is typical behaviour for aggregation of haematite, as the salt reduces the repulsive forces originating in the particle electrical double layers (see 22). The growth behaviour can be divided into three regions in each of which there is no strong dependence on particle concentration: for salt concentration below 30mM, the repulsive forces predominate and no growth occurs; concentrations between 30 and 50 mM show an increasing particle growth rate with salt concentration as the repulsion barrier is increasingly counterbalanced; above 50mM, with no repulsive forces, rapid coagulation takes place and particle growth becomes independent of salt concentration. Under the conditions used here, the critical coagulation concentration, at which repulsive forces are counterbalanced by Hamaker attractions, was found to be 40mM and 43 mM of KCl (see Fig. A1, A2) for the particle concentrations of Fig. 3 and 4, respectively. These values were used to estimate the Hamaker constant for the two sets of experiments, and were computed to be $2.43 \times 10^{-20} J$ and $2.37 \times 10^{-20} J$, respectively (see Appendix). If these results are used in eqn. [20], together with the reported value of $1.52 \times 10^{-19} J$ for the Hamaker constant of Haematite in vacuum (23), the resulting Hamaker constant for water is $5.4 \times 10^{-20} J$, which is well within the range of values found in the literature (see 12,22).

From the experimental conditions described above, theoretical curves were generated by numerical integration of the equations described in the "Theoretical Model" section. The computational method utilized was the Runge-Kutta-Gear routine and all the required physical constants were either supplied (i.e. η, k_B, T, etc.) or measured (i.e. zeta potential, Hamaker constant) with the exception of parameters defining the aggregate structure (i.e. packing factor f or fractal dimension d_F).

Consider firstly the use of a constant packing factor to define aggregate structure. The packing factor for regularly packed spheres is of the order of 0.7 (0.74 for Face Centered Cubic packing and 0.68 for Body Centered Cubic packing) (24). When such a value is used in the model calculations here, good correspondence between model and experiment is obtained (see Figure 5) under conditions where the aggregate size is small and an assumption of close packing likely to be reasonable (i.e at low salt concentration where the rate of aggregation is slow and at early times in systems forced to aggregate more rapidly through higher salt additions). However, a model incorporating a constant packing factor is clearly inappropriate for the rapidly aggregating system at later times where such a model is observed to grossly underpredict agglomerate size (Figure 5). In this case, a model incorporating increasing porosity with increasing size (a property characterictic of a fractal structure) might be expected to provide better correspondence with observation.

An estimate of the fractal dimension appropriate to the rapidly aggregating case (i.e salt concentrations greater than the critical coagulation) can be obtained by non linear least square curve fitting of the aggregate size versus time dependency since, under these conditions $R \sim t^{\frac{1}{d_F}}$ (25). The fractal dimension estimated from the curve fitting is 2.3 ± 0.1. Before using this fractal dimension in computation of aggregate size (and subsequent comparison with measured hydrodynamic size), it should be recognized that the dimension computed through Equation 25 is the radius of gyration (R_g) - a radius somewhat less than the outer radius (R_f) of an equivalent sphere (26). The hydrodynamic radius (R_h) obtained experimentally is also expected to be less than the outer radius for aggregates with density less than a solid sphere, but is not necessarily identical to the radius of gyration (R_g). In fact, the relationship between R_h and R_g is dependent on the nature of packing. For example, Chen and Meakin (27,28) obtained values for $\frac{R_h}{R_g}$ of 0.875 and 0.97 for simulated clusters with d_F=1.78 and 2.1 respectively. For a solid sphere (d_F=3), the $\frac{R_h}{R_g}$ ratio becomes $\sqrt{\left(\frac{5}{3}\right)}$. For $d_F = 2.3$ as found here, the radius of gyration and the hydrodynamic radius would be expected to be very similar and indeed the comparison of theoretical curves with experimental data (50mM KCl) in Figure 5 is good.

As introduced earlier, the apparent success of a fractal dimension in describing the rapid aggregation data suggests that, under these conditions, the aggregates become looser (less dense) as their size increases. This tendency can be quantified by equating equations [23] and [25], resulting in

$$f' = n^{1-\left(\frac{3}{d_F}\right)} \qquad [27],$$

(f' is used instead of f to avoid confusion with the constant packing factor used above). Equation [27] states that, for a fixed d_F, f' decreases with n, the number of particles in the aggregate. The variation of f' with n, for d_F=2.3 is shown graphically in Figure 6. It can be seen that for few particles, the value of f' is consistent with the packing factor of regularly packed spheres (i.e. $f' \approx 0.7$) but decreases as n increases.

The fractal dimension of 2.3 obtained here under rapid aggregation conditions (no repulsion barrier) is only slightly less than the value of 2.5 expected for aggregates growing via particle cluster diffusion limited aggregation (DLA) (29,30). In DLA, clusters grow purely from monomers, which approach the cluster with a random-walk trajectory. The random-walk nature of the approaching monomer favours growth on the extremities of the cluster, and thus, open, ramified geometries develop. Cluster-cluster aggregation (CA) is a variation of DLA where clusters grow from existing clusters as well as from monomers (31). In CA, d_F is reduced substantially because two fractals are extremely unlikely to penetrate without contact. Fractal dimensions on the order of 1.75 are to be expected where cluster-cluster aggregation is the dominant mechanism (32,33).

It can be seen from Figure 5 that an assumption of fractal dimension of 2.3 for the "low salt" case (30mM KCl) where aggregation is slow also gives close correspondence between computed and measured aggregate size. This is to be expected since, as mentioned above, a fractal structure for aggregates of small size (low particle numbers) is essentially identical to a regularly packed structure. It should also be noted that, under these conditions, the calculated aggregate size is relatively insensitive to the magnitude of d_F.

Measured and calculated aggregate sizes as functions of time for several salt concentrations and haematite concentrations of 4.5×10^{13} and 2.25×10^{13} particles/litre are shown in Figures 7 and 8 respectively. As discussed above, close correspondence between measured sizes and sizes calculated assuming a fractal dimension of 2.3 is observed both at salt concentrations above the critical coagulation concentrations (where aggregation is essentially a diffusion limited process) and at salt concentrations of sufficient magnitude to prevent significant aggregation occuring. However, in the intermediate region (salt concentration of 40mM in Fig. 7 and 30mM in Fig. 8), the sizes predicted with d_F are significantly larger than the experimentally measured sizes. It is implied from such an observation that the aggregate structure in this salinity region would be more appropriately described by a larger fractal dimension (i.e. more closely packed). Such an implication appears reasonable since, under the conditions determining intermediate (and slow) aggregation rates, the repulsion barrier is significant and the probability of sticking is low. The aggregating clusters will thus have the opportunity to explore a large number of possible structural configurations leading to some interpenetration and thus denser aggregates i.e. higher fractal dimension). Further details on the variation in fractal dimension with rate of aggregation of haematite are presented elsewhere (34).

It should be recognized that, in calculating the stability ratio (i.e. in computation of repulsive and attractive forces), a solid particle with an equivalent spherical size accounting for the fractal nature of the aggregate is assumed. For low salt concentration, the number of primary particles in the aggregates is low and these particles are closely packed. As discussed above, the deduced fractal dimension of 2.3 would also give a packed structure for aggregates containing a small number of particles. This suggests that use of an equivalent spherical size in calculating the stability ratio under these conditions is reasonable. For high salt concentrations, the aggregates are more loosely packed and contain large numbers of primary particles. Use of an equivalent sphere in computation of repulsive and attractive forces under these conditions might be expected to generate deviations between observed and predicted results. However, at these salt concentrations, the

effect of repulsive force is not significant; the aggregation is mainly due to diffusion. It is only in the intermediate regime where the repulsive force is still significant, but the aggregates are not closely packed, that description of the encounter of objects with fractal character using equations derived for the estimation of interactive forces between spherical particles may introduce some errors.

CONCLUSIONS

In this work, the kinetics of growth of haematite has been determined by direct measurement of aggregate size utilizing Photon Correlation Spectroscopy. Growth tests were performed by varying the ionic strength of the medium and the effect observed was typical: slow agglomeration for small salt concentration (up to 30mM of KCl); transition region for KCl concentration between 30 and 50mM, and rapid aggregation for salt concentration above 50mM. A theoretical model, derived from the Smoluchowski equation modified to account for the repulsion and attraction energies during aggregation and for the packing characteristics of the aggregate, was developed and compared with the experimental results. The resulting comparisons indicate that the aggregates have a fractal structure with their packing becoming looser as their size increases. A fractal dimension of 2.3 yields aggregate sizes that correspond closely to measured sizes for salt concentrations greater than the critical coagulation concentration (i.e. in the rapid aggregation region). This value is slightly less than expected for particle-cluster diffusion limited aggregation (DLA) and suggests that a combination of DLA and cluster-cluster aggregation (CA) is occuring. Not surprisingly, use of d_F=2.3 in the region of intermediate aggregation kinetics results in over prediction of aggregate sizes. Closer packing (larger d_F) is to be expected in this region of retarded aggregation because of the opportunity for interacting aggregates to find lower energy interpenetrated structures.

REFERENCES

(1) B.E. Novich and T.A. Ring, J. Chem. Soc. Faraday Trans., **81** (1985) 1455.

(2) M. Smoluchowski, Z. Phys. Chem., **92** (1917) 129.

(3) B. Chu, Laser Light Scattering, Academic Press, New York, 1974.

(4) H.Z. Cummings and P.N. Pusey in H.Z. Cummings and E.R. Pike (Eds.), Photon Correlation Spectroscopy and Velocimetry, Plenum, New York, 1977,pp. 164-199.

(5) R. Pecora, in B.E. Dahneke (Ed.), Measurement of Suspended Particles by Quasi-Elastic Light Scattering, Wiley, New York, 1983, pp 3.

(6) D.E. Koppel, J. Chem. Phys., **57** (1972) 4814.

(7) J.C. Brown and P.N. Pusey, J. Chem. Phys., **62** (1975) 1136.

(8) A. Sheludko, Colloid Chemistry, Elsevier Publishing Company, 1966.

(9) N. Füchs, Z. Phys., **89** (1934) 736.

(10) R. Hogg, T.W. Healy and D.W. Fuerstenau, Trans. Faraday Soc., **62** (1966) 1638.

(11) H.C. Hamaker, Physica, **4** (1937) 1058.

(12) J.N. Israelachvilli and G.E. Adams, J.Chem.Soc. Faraday Trans. 1, **60** (1974) 1675.

(13) E.A. Barringer, B.E. Novich and T.A. Ring, J. Colloid and Interface Sci., **100** (1984) 584.

(14) D.A. Weitz, M.Y. Lin and C.J. Sandroff, Surf. Sci., **158** (1985) 147.

(15) E. Matijevic and P. Scheiner, J. Colloid and Interface Sci., **63** (1978) 509.

(16) N.H.G. Penners and L.K. Koopal, Colloids and Surfaces, **19** (1986) 337

(17) R. Amal, J.R. Coury, J.A Raper and T.D. Waite,in The Institution of Chemical Engineers 5th International Synposium on AGGLOMERATION, 25-27 September 1989, Brighton Conference Centre, UK.

(18) Lord Rayleigh, Proc. Roy. Soc., **A90** (1914) 219.

(19) R. Gans, Ann. Physik., **37** (1912) 881.

(20) G. Mie, Ann. Physik., **25** (1908) 378.

(21) P. Hiemenz, Principles of Colloid and Surface Science, Dekker, New York, 1977.

(22) D.J. Shaw, Introduction to Colloid and Surface Chemistry, Butterworths, 1980.

(23) J. Lyklema, Advan. Colloid Interface Sci., 2 (1968) 65.

(24) D. Hayes, Kinetic Studies on Colloidal Systems, Ph.D. Thesis, University of Melbourne, (October 1987).

(25) D.A. Weitz and J.S. Huang, in F. Family and D.P. Landau (Eds.), Proc. Intern. Topical Conf. on the Kinetics of Aggregation and Gelation, North-Holland, Amsterdam, 1984, pp. 19.

(26) J. Feder, Fractals, Plenum Press, New York, 1988.

(27) P. Meakin, Z.Y. Chen and J.M. Deutch, J. of Chem. Phys., **82** (1985) 3786.

(28) Z.Y. Chen, P. Meakin and J.M. Deutch, Phys. Rev. Lett., **59** (1987) 2121.

(29) T.A. Witten and L.M. Sander, Phys. Rev. Lett., **47** (1981) 1400.

(30) P. Meakin, Phys. Rev. A, **27** (1983) 1495.

(31) D.W. Schaefer and J.E. Martin, Phys. Rev. Lett., **52** (1984) 2371.

(32) P. Meakin, Phys. Rev. Lett., **51** (1983) 1119.

(33) M. Kolb, R. Botet and J. Jullien, Phys. Rev. Lett., **51** (1983) 1123.

(34) R. Amal, J.A. Raper and T.D. Waite, J. Colloid Interface Sci. (submitted).

APPENDIX

The rate of aggregation in the initial stage of aggregation assuming irreversible transformation of singlets to doublets can be written as,

$$\frac{dn_1}{dt} = -k_s n_1^2 \qquad [A1].$$

If the fraction of singlets converted is equal to x, fraction of doublets formed is $\frac{1}{2}x$, and the total remaining fraction is $1-\frac{1}{2}x$ with respect to initial total number of particles. The average size at certain x can be expressed according to Eq. [26] as,

$$R = \frac{\left(\frac{1-x}{1-1/2x}\right)R_1^4 + \left(\frac{1/2x}{1-1/2x}\right)R_2^4}{\left(\frac{1-x}{1-1/2x}\right)R_1^3 + \left(\frac{1/2x}{1-1/2x}\right)R_2^3} \qquad [A2],$$

where R_1 is the size of singlet, and R_2 is the size of doublet. R_2 can then be related to R_1,

$$R_2 = c \times R_1 \qquad [A3],$$

where c is a constant. By rearranging and simplifying Eq. [A2], x becomes

$$x = \frac{R - R_1}{(1 - 1/2f^3)R - (1 - 1/2f^4)R_1} \qquad [A4].$$

If it is assumed that $x \to 0$ as $t \to 0$ plotting x versus time would give $k_s n_0$ as the slope at $t \to 0$.

After obtaining k_s from the slope, the stability ratio (W) curve, i.e. plot of ln(W) vs ln(salt concentration) can be drawn, which then will give the critical coagulation concentration (the experimental results for this work are plotted in Fig. A1,A2). At critical coagulation concentration, the total interaction energy and its first derivative are zero. Therefore, the total interaction energy (V_T), for $\psi_i = \psi_j = \psi$, becomes:

$$V_T(H) = \frac{\pi\varepsilon_0\varepsilon_R r_1 r_2}{r_1 + r_2}\psi^2 \ln\{1 + \exp(-\kappa H)\}$$

$$-\frac{A}{12}\left\{\frac{y}{x^2+xy+x} + \frac{y}{x^2+xy+x+y} + 2\ln\left\{\frac{x^2+xy+x}{x^2+xy+x+y}\right\}\right\} = 0 [A6]$$

and its first derivative,

$$\frac{dV_T(H)}{dH} = \frac{\pi\varepsilon_0\varepsilon_R r_1 r_2}{r_1 + r_2}\psi^2\left(\frac{-\kappa\exp(-\kappa H)}{1+\exp(-\kappa H)}\right)$$

$$-\frac{A\left(\frac{x}{r_1}+\frac{y}{r_1}+\frac{1}{2r_1}\right)}{12}\left\{\frac{2(x^2+xy+x)-y}{(x^2+xy+x)^2} - \frac{2(x^2+xy+x+y)+y}{(x^2+xy+x+y)^2}\right\} = 0 [A7].$$

By solving equations [A6] and [A7] simultaneously, the effective Hamaker constant can be obtained. For the first set of data, the effective Hamaker constant was $2.43 \times 10^{-20} J$, while the second set of data gave $2.37 \times 10^{-20} J$.

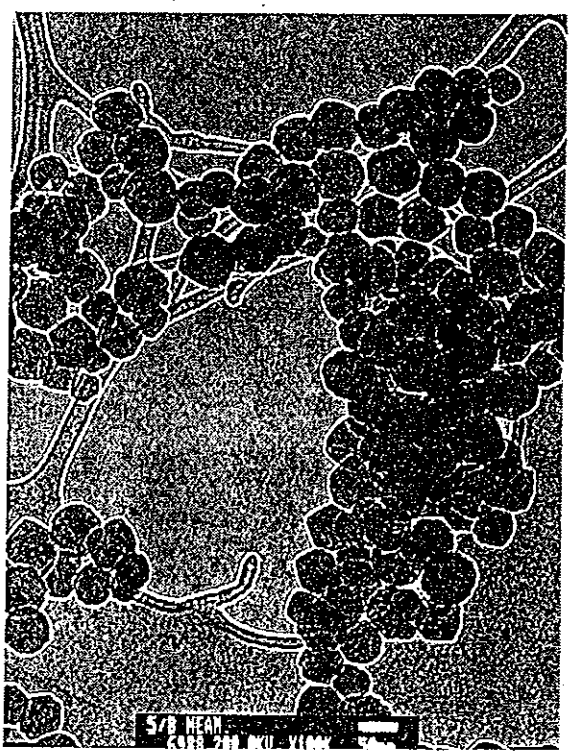

Figure 1. Representative Transimission Electron Micrograph (TEM) of haematite particles.

Figure 2. Typical result obtained from Malvern 4700 Photon Correlation Spectrometer.

Live Data from Correlator
Temperature 25.0 Viscosity 0.8905 Refractive Index 1.330 Angle 90.0

Particle size distribution (nm.)			Graph of Intensity distribution
9.2	-	11.1	+ +
11.1	-	13.4	+ +
13.4	-	16.3	+ +
16.3	-	19.7	+ +
19.7	-	23.9	+ +
23.9	-	28.9	+ +
28.9	-	35.1	+ +
35.1	-	42.5	+ +
42.5	-	51.5	+ +
51.5	-	62.3	--+ +
62.3	-	75.5	----------+ +
75.5	-	91.5	----------+ +
91.5	-	110.9	----------+ +
110.9	-	134.3	----------+ +
134.3	-	162.7	----------+ +
162.7	-	197.2	----------+ +
197.2	-	238.9	----------+ +
238.9	-	289.4	----+ +
289.4	-	350.6	+ +
350.6	-	424.8	+ +
424.8	-	514.6	+ +
514.6	-	623.5	+ +
623.5	-	755.3	+ +
755.3	-	915.1	+ +

Size		Class	% by Intensity			% by mass			% by number		
			Under	In	Above	Under	In	Above	Under	In	Above
9.2	-	11.1	0.0	0.0	100.0	0.0	0.0	100.0	0.0	0.0	100.0
11.1	-	13.4	0.0	0.0	100.0	0.0	0.0	100.0	0.0	0.0	100.0
13.4	-	16.3	0.0	0.0	100.0	0.0	0.0	100.0	0.0	0.0	100.0
16.3	-	19.7	0.0	0.0	100.0	0.0	0.0	100.0	0.0	0.0	100.0
19.7	-	23.9	0.0	0.0	100.0	0.0	0.0	100.0	0.0	0.0	100.0
23.9	-	28.9	0.0	0.0	100.0	0.0	0.0	100.0	0.0	0.0	100.0
28.9	-	35.1	0.0	0.0	100.0	0.0	0.0	100.0	0.0	0.0	100.0
35.1	-	42.5	0.0	0.0	100.0	0.0	0.0	100.0	0.0	0.0	100.0
42.5	-	51.5	0.0	0.0	100.0	0.0	0.0	100.0	0.0	0.0	100.0
51.5	-	62.3	0.0	1.0	99.0	0.0	7.7	92.3	0.0	23.7	76.3
62.3	-	75.5	1.0	7.0	92.0	7.7	19.6	72.6	23.7	33.9	42.5
75.5	-	91.5	8.0	18.5	73.5	27.4	26.2	46.5	57.5	25.4	17.1
91.5	-	110.9	26.5	19.1	54.4	53.5	21.0	25.4	82.9	11.5	5.6
110.9	-	134.3	45.6	19.9	34.5	74.6	13.0	12.5	94.4	4.0	1.7
134.3	-	162.7	65.5	17.1	17.3	87.5	7.3	5.2	98.3	1.3	0.4
162.7	-	197.2	82.7	10.4	7.0	94.8	3.4	1.8	99.6	0.3	0.1
197.2	-	238.9	93.0	5.2	1.8	98.2	1.3	0.4	99.9	0.1	0.0
238.9	-	289.4	98.2	1.8	0.0	99.6	0.4	0.0	100.0	0.0	0.0
289.4	-	350.6	100.0	0.0	0.0	100.0	0.0	0.0	100.0	0.0	0.0
350.6	-	424.8	100.0	0.0	0.0	100.0	0.0	0.0	100.0	0.0	0.0
424.8	-	514.6	100.0	0.0	0.0	100.0	0.0	0.0	100.0	0.0	0.0
514.6	-	623.5	100.0	0.0	0.0	100.0	0.0	0.0	100.0	0.0	0.0
623.5	-	755.3	100.0	0.0	0.0	100.0	0.0	0.0	100.0	0.0	0.0
755.3	-	915.1	100.0	0.0	0.0	100.0	0.0	0.0	100.0	0.0	0.0

z Average Mean 100.6 Poly 0.182 Dist. mean 124.2 St.Dev. 43.3
Analysis range 100 : fit : 0.0252

Run	: counts/1000	: % merit	: % in-range:	Count rate 1000's/sec
1	3153.2	56.0	97.8	286.6

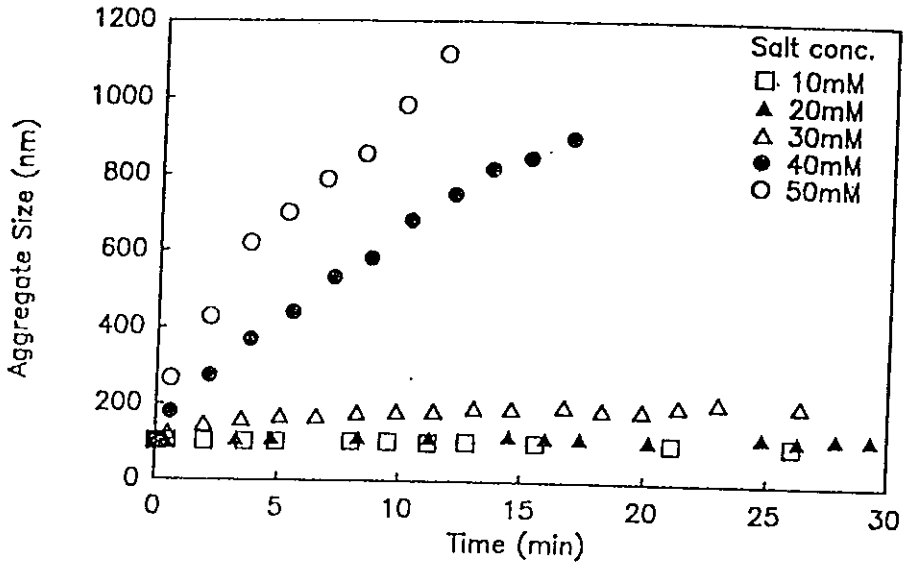

Figure 3. The aggregation curves of haematite particles (4.5×10^{13} particles/liter) with different salt concentrations.

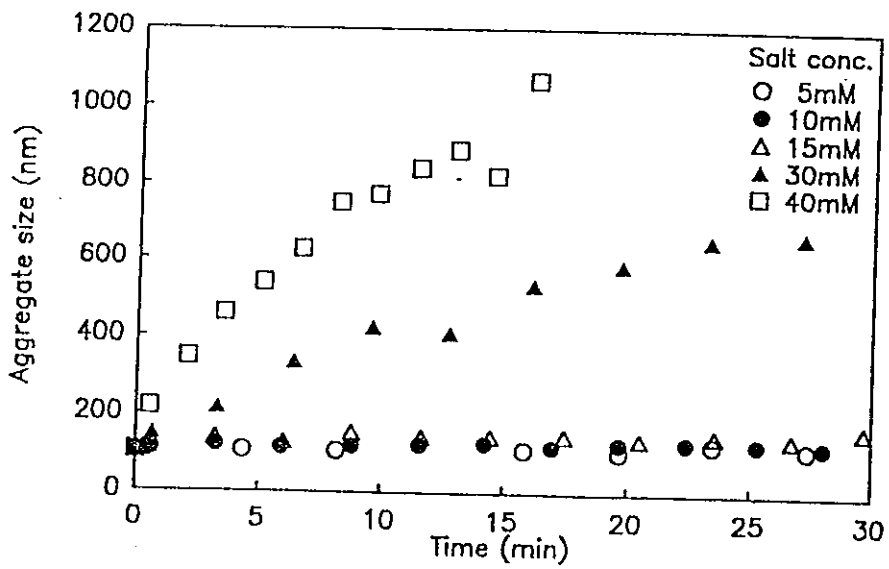

Figure 4. The aggregation curves of haematite particles (2.25×10^{13} particles/liter) with different salt concentrations.

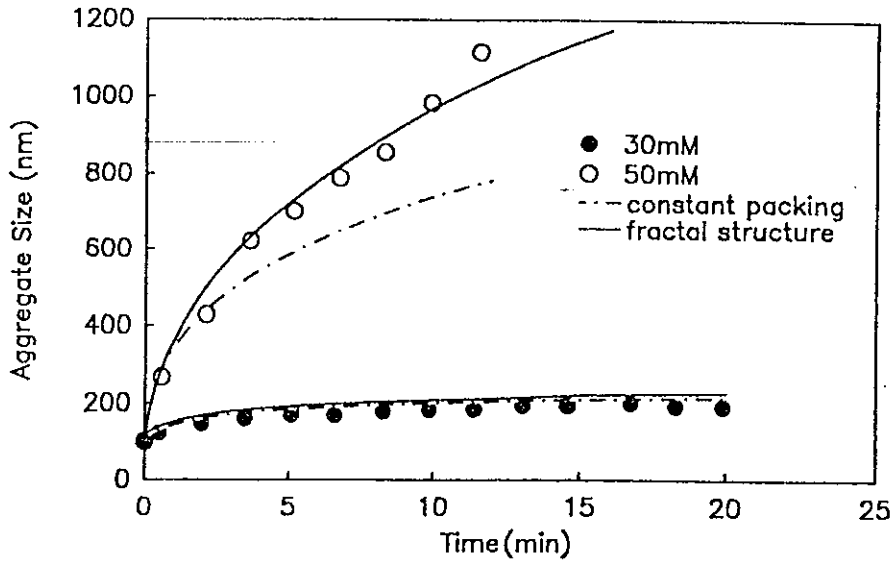

Figure 5. Comparison of constant packing and fractal structure models for slow (30mM KCl) and rapid (50mM KCl) aggregation.

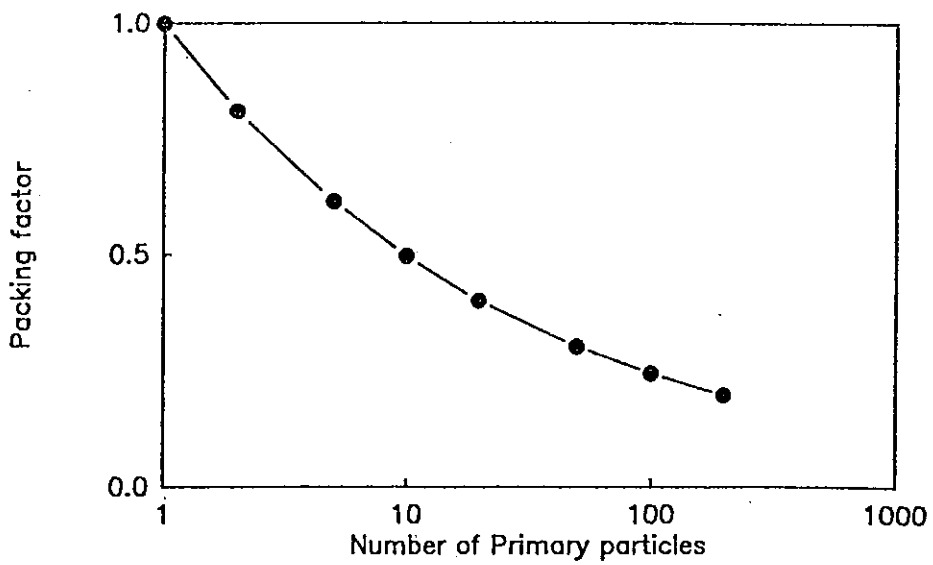

Figure 6. The variation of the packing factor with increasing number of particles, n, in the fractal structure.

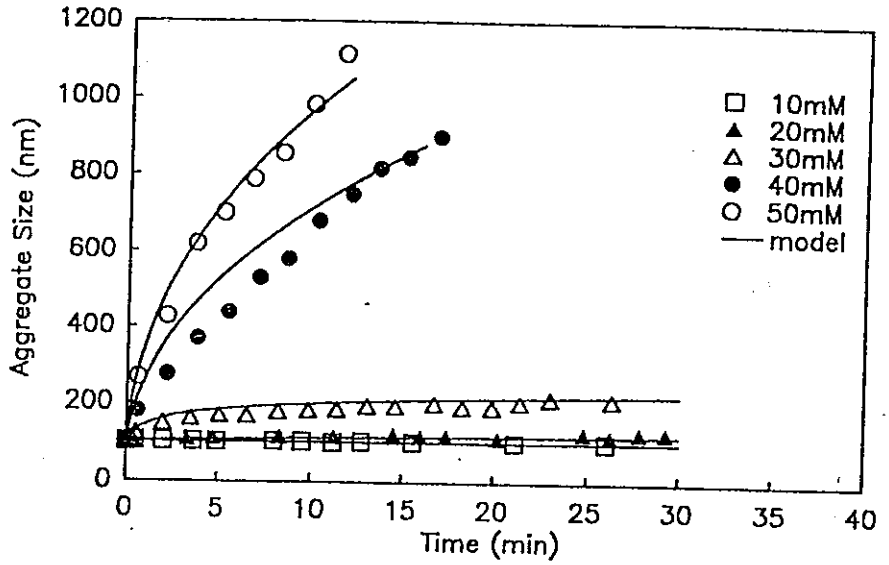

Figure 7. Comparison of the fractal structure model with the experimental data for particle concentration of 4.5×10^{13} particles/liter.

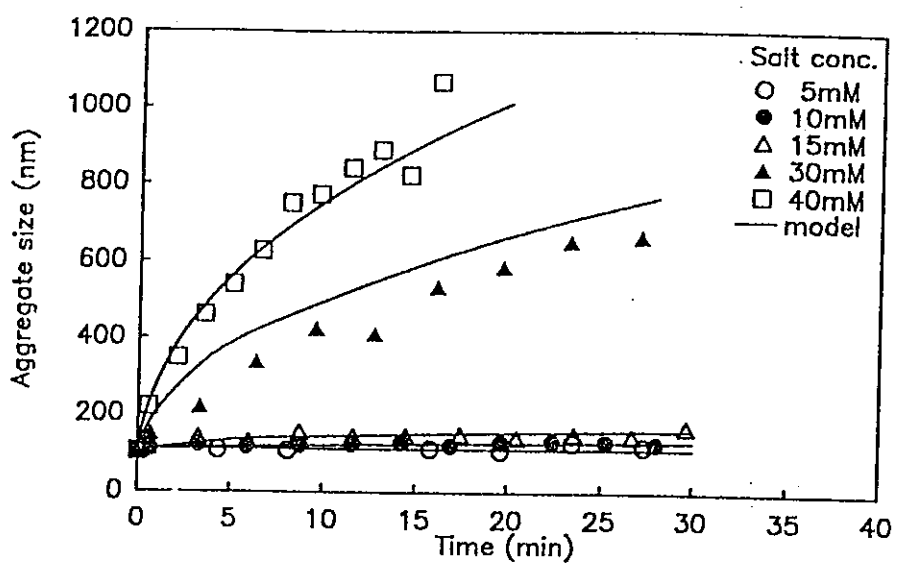

Figure 8. Comparison of the fractal structure model with the experimental data for particle concentration of 2.25×10^{13} particles/liter.